Energy Conversion by Semiconductor Devices

Jun-Ho YUM
junho.yum@epfl.ch

Halide Perovskite

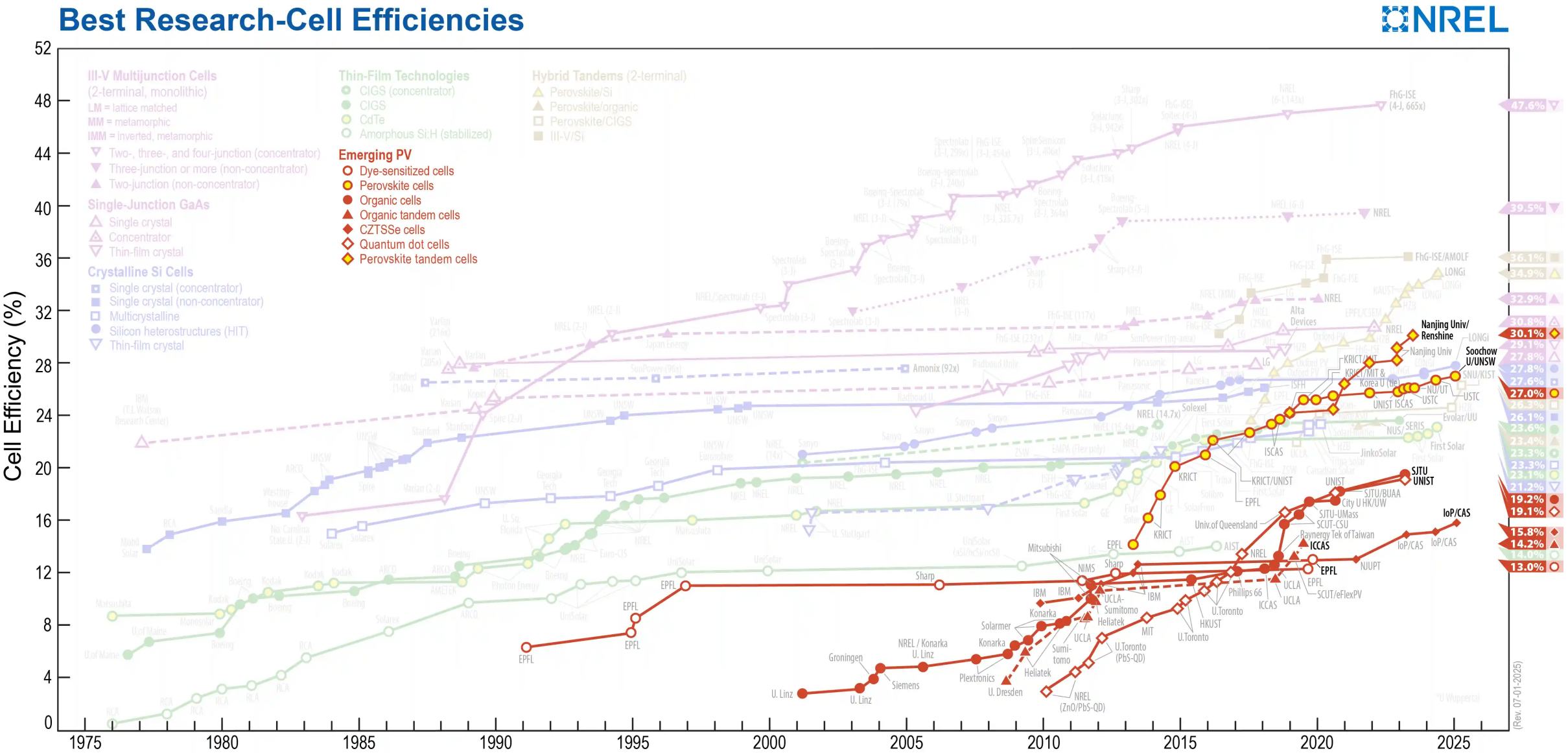

27.0%

- Jun-Ho YUM, junho.yum@epfl.ch

What is Perovskite?

- 1839: perovskite = $CaTiO_3$ discovered

- 1958: $CsPbX_3$ (X = Cl, Br, or I) perovskite structure determined

Møller, C. K. *Nature* **182,** 1436 (1958).

- 1978 Cs cation replaced by methylammonium cations $CH_3NH_3^+$ → organic–inorganic hybrid perovskites

Weber, D. *Z. Naturforsch.* **33b,** 1443–1445 (1978).
Weber, D. *Z. Naturforsch.* **33b,** 862–865 (1978).

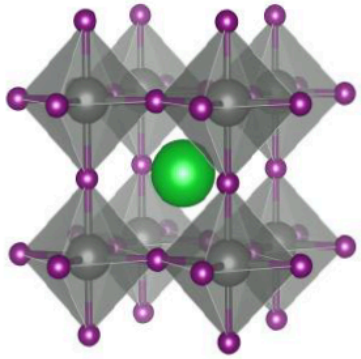

- Last two decades: perovskite researched in electronics

D. B. Mitzi, *Progress in Inorganic Chemistry* Vol. 48 (ed. Karlin, K. D.) 1–121 (J. Wiley & Sons, 1999).
T. Ishihara, *Journal of Luminescence* **60–61,** 269–274 (1994).

What is Perovskite for Solar Cells?

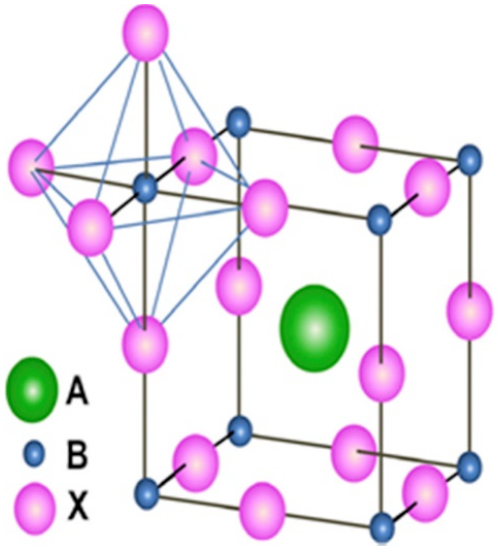

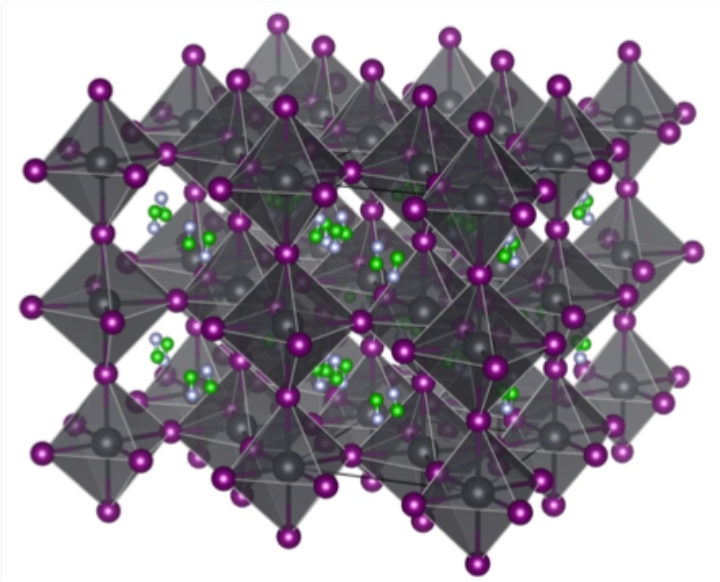

ABX_3:

A (green) is a large metal cation such as Cs^+, $CH_3NH_3^+$, $HC(NH_2)_2^+$

B (blue) is a small metal cation such as Pb^{2+}, Sn^{2+}

X (purple) is Cl^-, Br^-, I^-

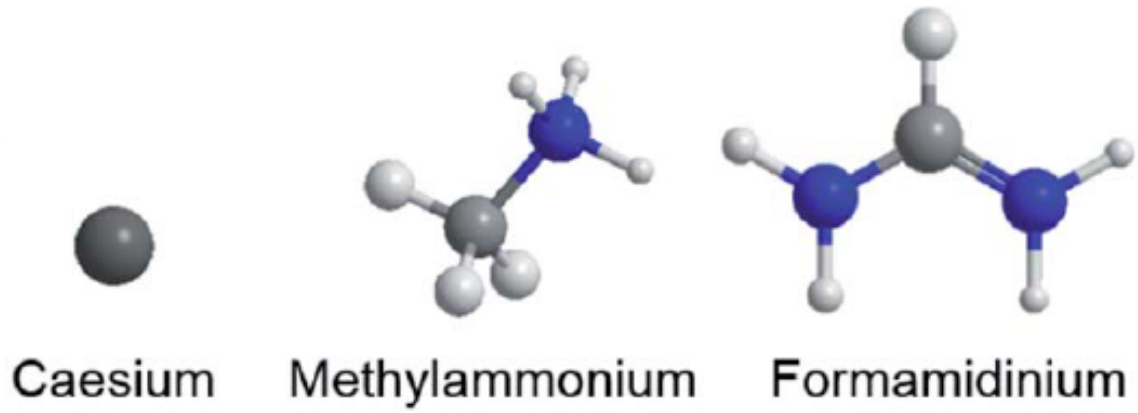

Mono-cation: $CH_3NH_3PbI_3$ ($MAPbI_3$ or MALI), $HC(NH_2)_2PbI_3$ ($FAPbI_3$), $CsPbI_3$

Multi-cations: $MA_xFA_{1-x}PbI_3$, $Cs_xFA_{1-x}PbI_3$, $Cs_xMA_yFA_{1-x-y}PbI_3$ ($CsMAFAPbI_3$)

Multi-anions: $MAPb(I_xBr_{1-x})_3$, $MAPb\ (I_xCl_{1-x})_3$

Jun-Ho YUM, junho.yum@epfl.ch

Goldschmidt Tolerance Factor & Octahedral Factor

In the typical ABX_3, the crystallographic stability and probable structure can be deduced by considering a Goldschmidt tolerance factor *t* and and octahedral factor μ.

The A cation can fit within the BX_3 framework of corner sharing octahedra.
The range from 0.8 to 1 indicates perovskite formation (*t* = 1 indicates a perfect fit).

$$t = \frac{R_A + R_X}{\sqrt{2}(R_B + R_X)}$$

The B site cation can fit in the octahedral hole in the anion sublattice.
The radius of an octahedral hole formed within six close packed spheres of radius (R_{hole}) = $0.41R_X$

$$0.44 < \mu = \frac{R_B}{R_X} < 0.90$$

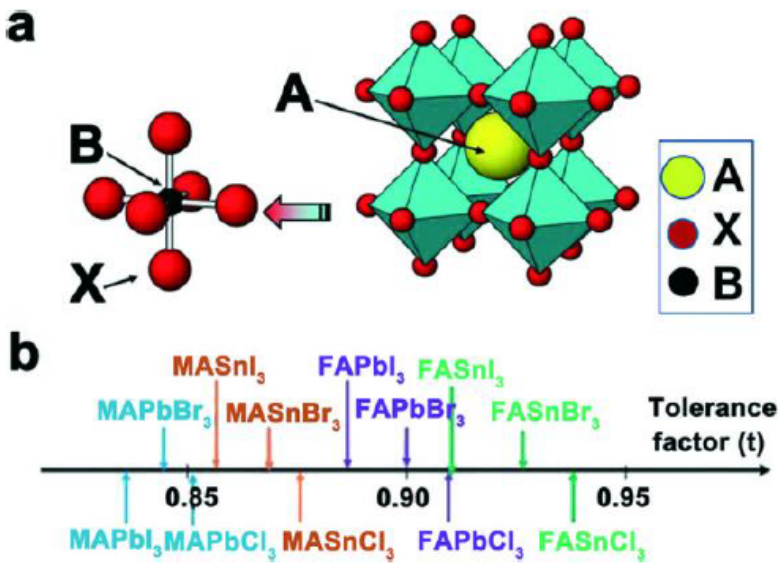

Z. Fan et al., *J. Mater. Chem. A,* **3**, 18809–18828 (2015).

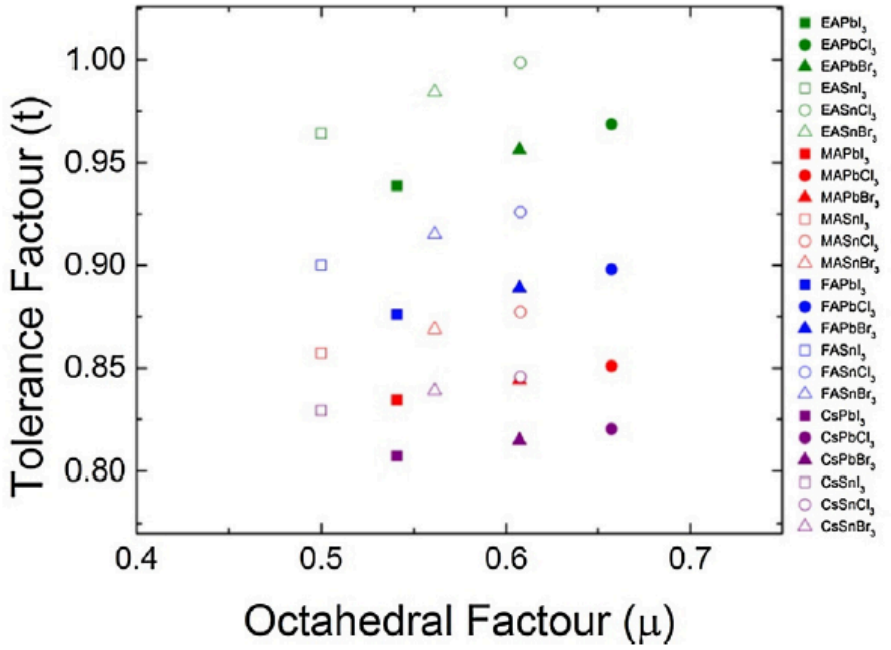

Q. Chen et al., *Nano Today,* **10**, 255–396 (2015).

Goldschmidt Tolerance Factor & Octahedral Factor

In the typical ABX_3, the crystallographic stability and probable structure can be deduced by considering a Goldschmidt tolerance factor *t* and and octahedral factor μ.

The A cation can fit within the BX_3 framework of corner sharing octahedra.
The range from 0.8 to 1 indicates perovskite formation (*t* = 1 indicates a perfect fit).

$$t = \frac{R_A + R_X}{\sqrt{2}(R_B + R_X)}$$

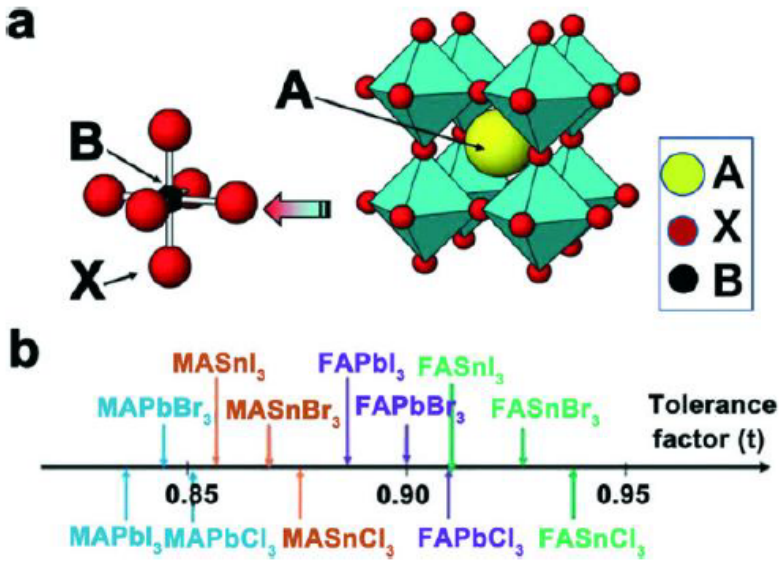

Z. Fan et al., *J. Mater. Chem. A,* **3**, 18809–18828 (2015).

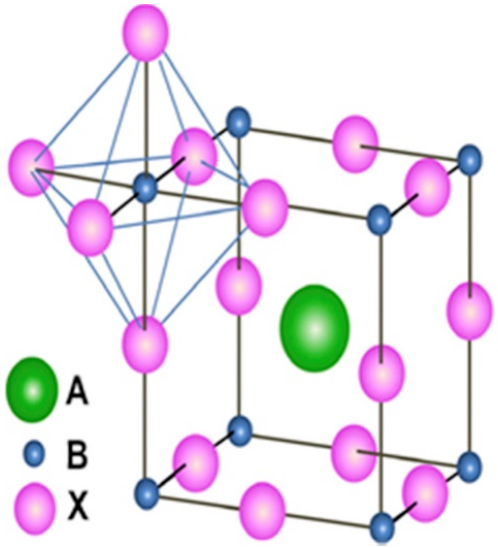

BX_3 framework
B = 1/8 x 8
X = 1/4 x 12

Goldschmidt Tolerance Factor & Octahedral Factor

In the typical ABX_3, the crystallographic stability and probable structure can be deduced by considering a Goldschmidt tolerance factor *t* and and octahedral factor μ.

The A cation can fit within the BX_3 framework of corner sharing octahedra.
The range from 0.8 to 1 indicates perovskite formation (*t* = 1 indicates a perfect fit).

$$t = \frac{R_A + R_X}{\sqrt{2}(R_B + R_X)}$$

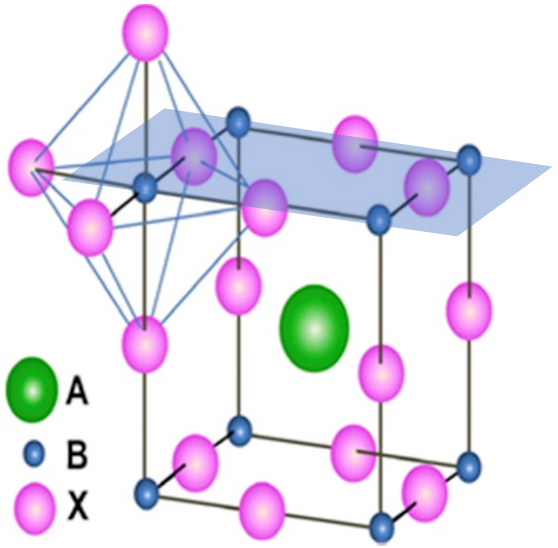

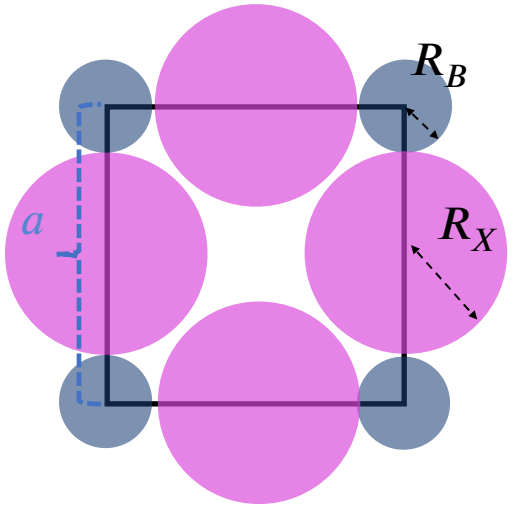

$$a = 2R_B + 2R_X$$

Goldschmidt Tolerance Factor & Octahedral Factor

In the typical ABX_3, the crystallographic stability and probable structure can be deduced by considering a Goldschmidt tolerance factor *t* and and octahedral factor μ.

The A cation can fit within the BX_3 framework of corner sharing octahedra.
The range from 0.8 to 1 indicates perovskite formation (*t* = 1 indicates a perfect fit).

$$t = \frac{R_A + R_X}{\sqrt{2}(R_B + R_X)}$$

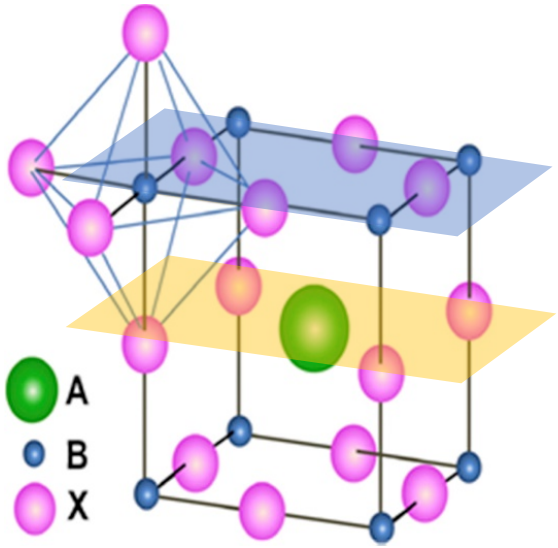

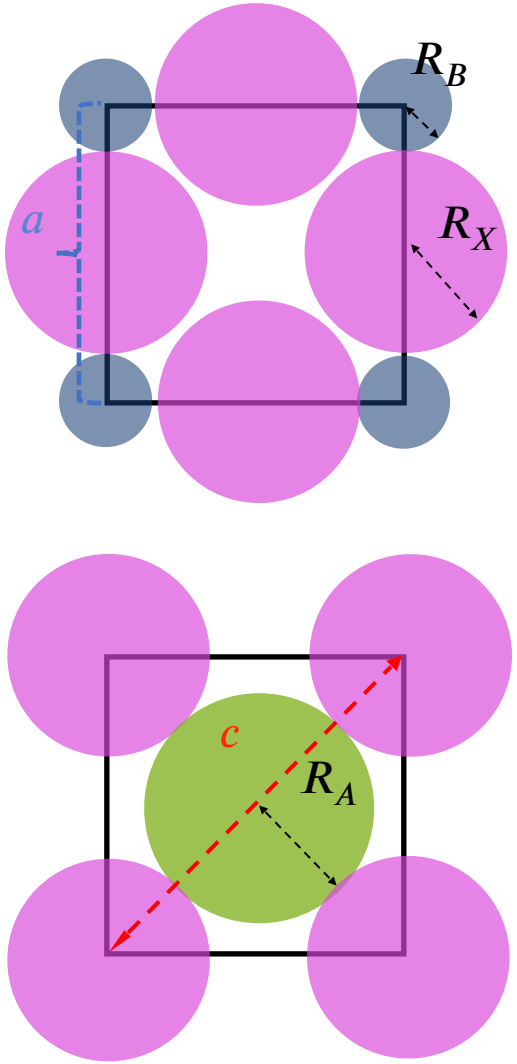

$$a = 2R_B + 2R_X$$

$$\frac{1}{cos45°} = \frac{c}{a}$$

$$t = \frac{c}{\sqrt{2}a}$$

$$c = 2R_A + 2R_X$$

Goldschmidt Tolerance Factor & Octahedral Factor

In the typical ABX_3, the crystallographic stability and probable structure can be deduced by considering a Goldschmidt tolerance factor *t* and and octahedral factor μ.

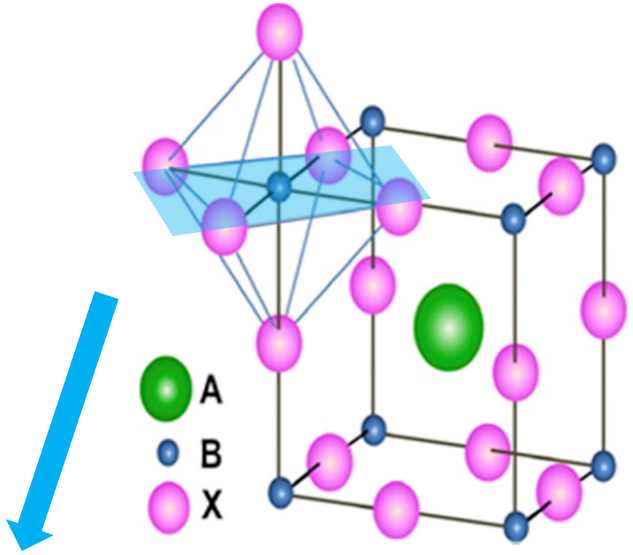

The B site cation can fit in the octahedral hole in the anion sublattice.
The radius of an octahedral hole formed within six close packed spheres of radius (R_{hole}) = *0.41*R_X

$$0.44 < \mu = \frac{R_B}{R_X} < 0.90$$

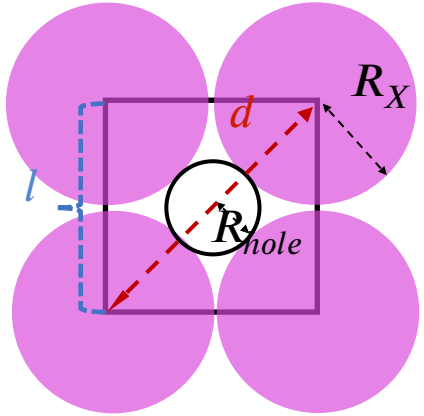

$$l = 2R_X$$

$$d = 2R_{hole} + 2R_X = \sqrt{2} \times l$$

$$2R_{hole} + 2R_X = \sqrt{2} \times 2R_X$$

$$R_{hole} = (\sqrt{2} - 1)R_X$$

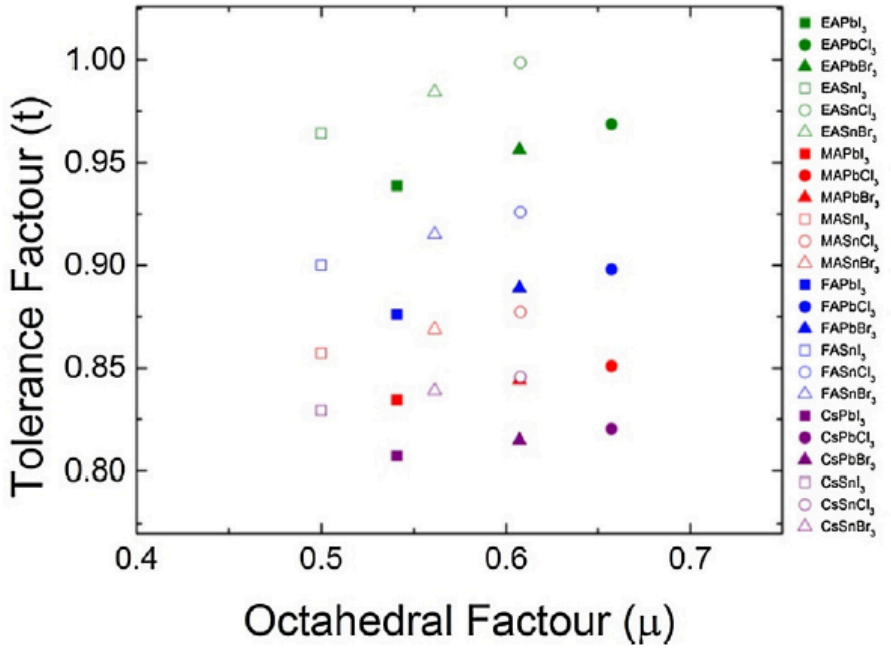

Q. Chen et al., *Nano Today,* **10**, 255–396 (2015).

Organic-Inorganic Halide Perovskite

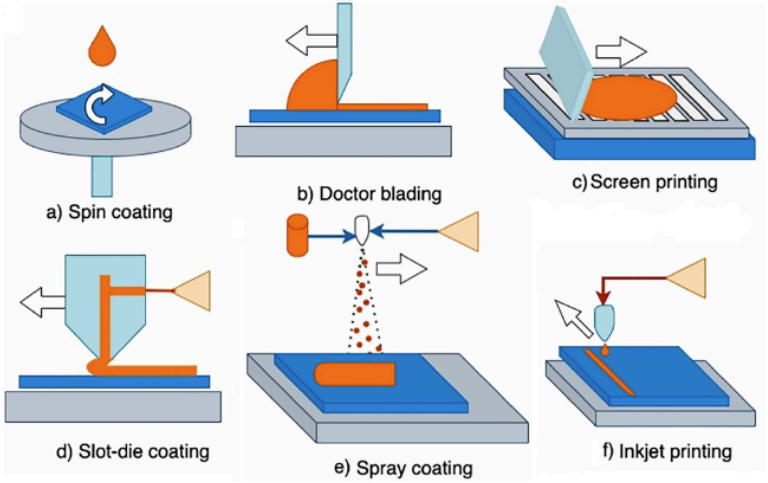

R. Afre et al., *Micromachines,* **15**, 192 (2024).

$MAPb(I_{1-x}Br_x)_3$

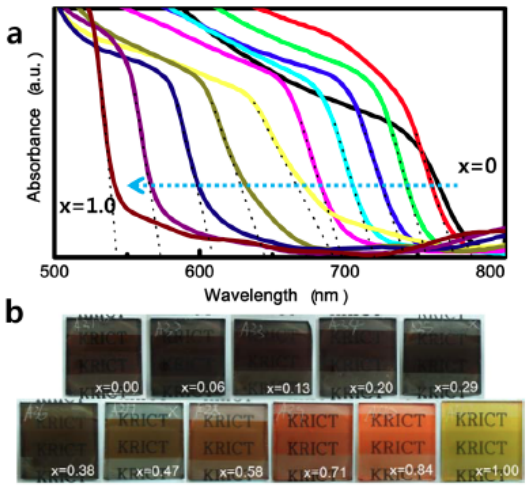

J.H. Noh et al., *Nano Lett,* **13**, 1764 (2013).

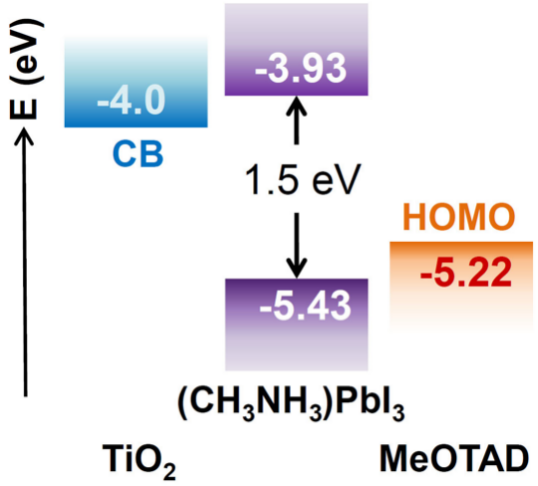

- **High crystallinity and low defect density, even if solution processed**
- **Absorption coefficient of 10^4 – 10^5 cm^{-1} (absorption depth = 100 - 1000 nm)**
- **Band gap of 1.6 eV and tunable band gap by compositional tuning**
- **Proper energy levels to be compatible with existing ETM and HTM**
- **Ambipolar semiconductor with high charge carrier mobilities (10 – 100 $cm^2V^{-1}s^{-1}$)**
- **Low exciton binding energy with fast dissociation at room temperature, high dielectric constant**

Band Gap Tuning

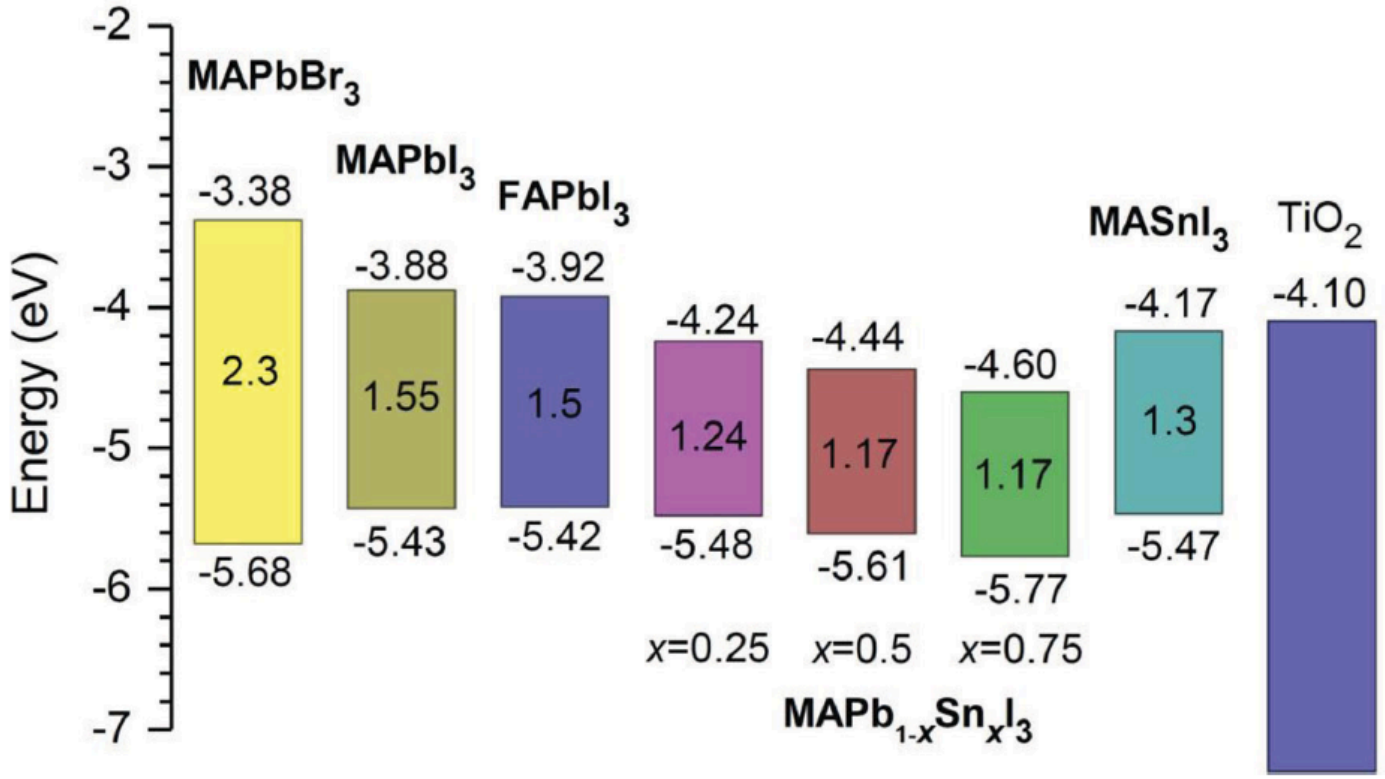

F. Hao et al., *J. Am. Chem. Soc.*, **136**, 8094 (2014).

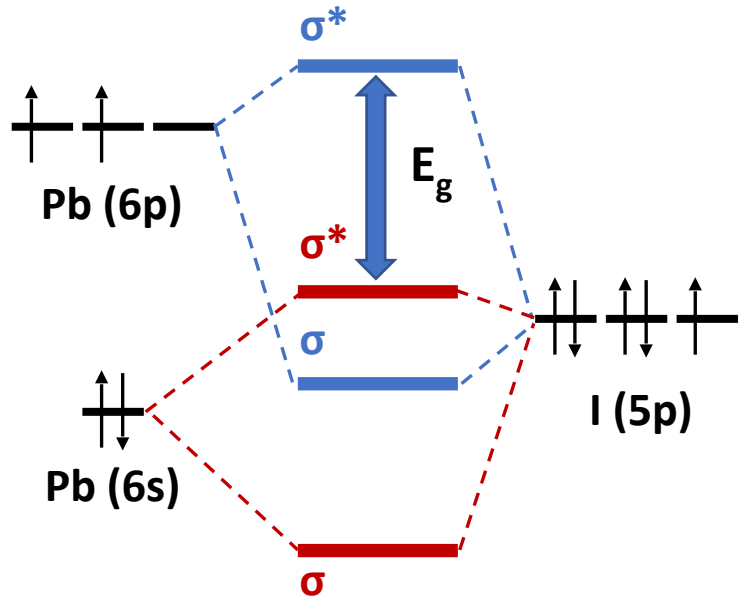

- **CB formed by the antibonding combination of empty Pb 6p (Sn 5p) orbitals.**
- **VB formed by the overlap of Pb 6s (Sn 5s) orbitals and X halogen np orbitals.**

Band Gap Tuning with X Anion

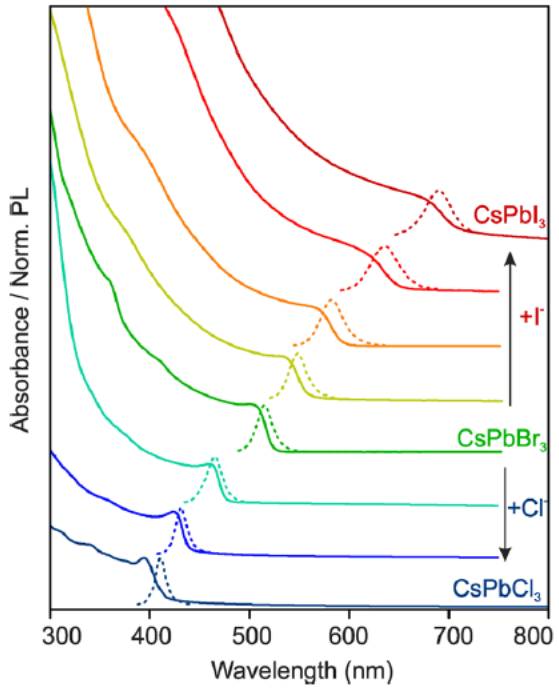

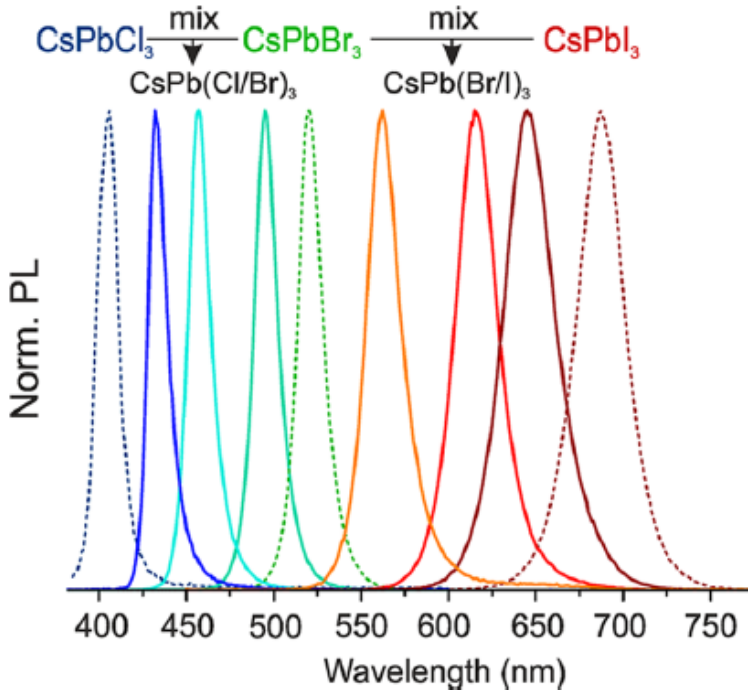

G. Nedelcu et al., , *Nano Lett.*, **15**, 5635 (2015).

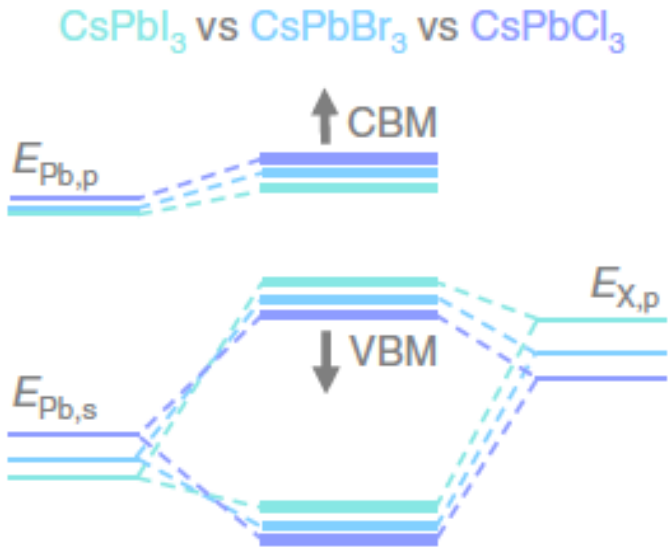

S. Tao et al., *Nature Commun.*, 10:2560 (2019).

- **The energy of the CBM is mostly influenced by the position of the Pb p orbital.**
- **A small shift in CBM is associated with that as the Pb-X distances decrease going from I to Br to Cl, an electron on a Pb atom is more confined and its energy increases (reason of the upward shift of Pb p and s orbitals).**
- **A significant downward shift of the X p orbital level going from I to Br to Cl, which simply reflects increasing electronegativity.**

Band Gap Tuning with X Anion

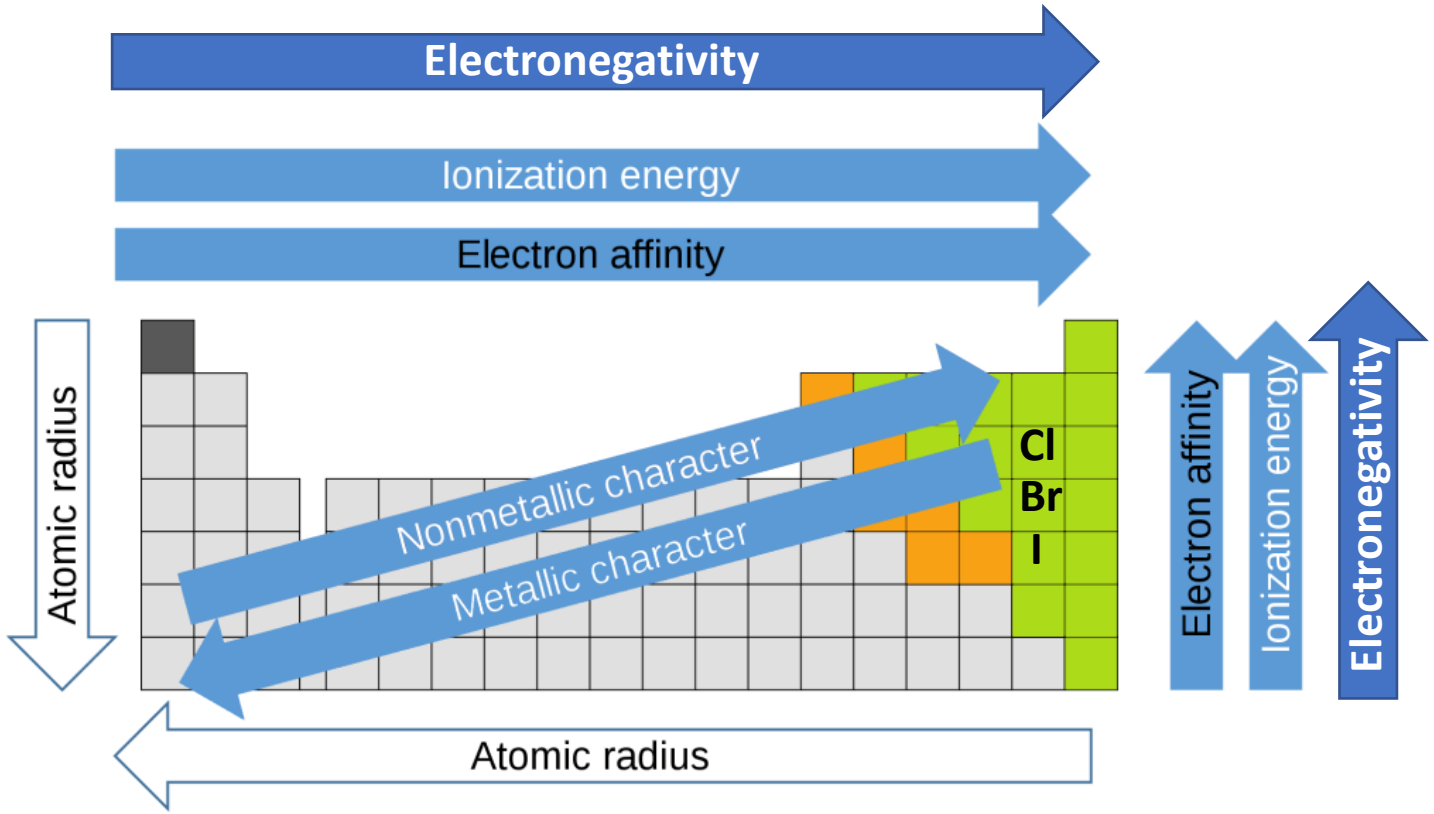

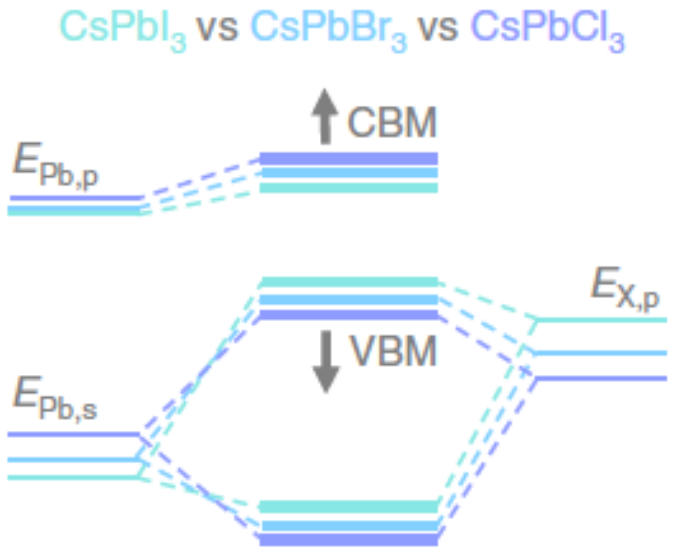

S. Tao et al., *Nature Commun.*, 10:2560 (2019).

Electronegativity is defined as an atom's ability to attract electrons towards it in a chemical bond.

Band Gap Tuning with B Cation

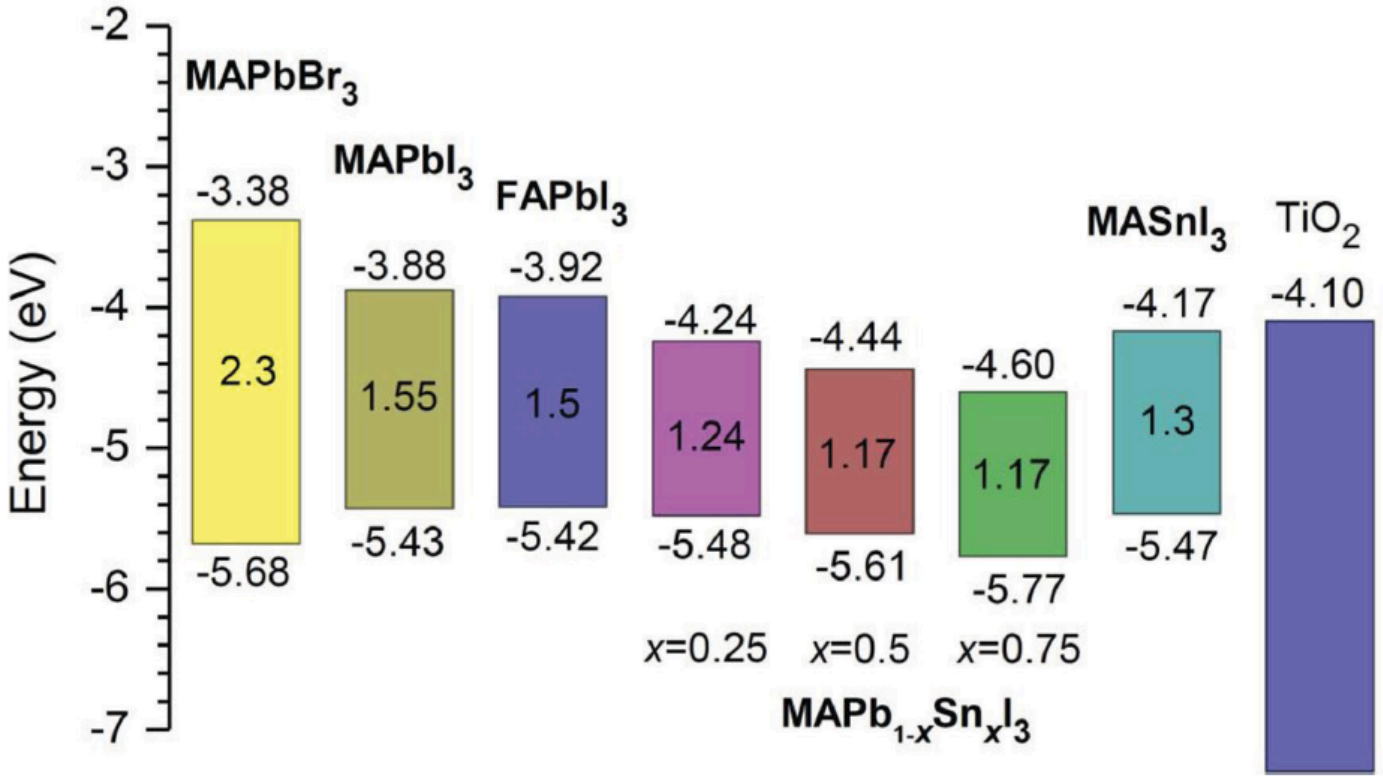

F. Hao et al., *J. Am. Chem. Soc.*, **136**, 8094 (2014).

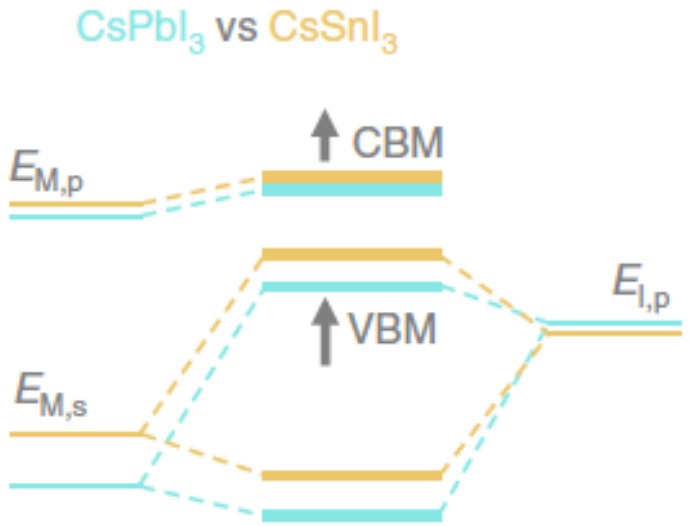

S. Tao et al., *Nature Commun.*, 10:2560 (2019).

- **Replacing Pb with Sn, the atomic levels shift upwards, which is consistent with the smaller electronegativity of Sn.**
- **The splitting between s and p states in a Sn atom is smaller than in a Pb atom due to a smaller spin-orbit coupling: the VBM shifts upward more than the CBM.**

Band Gap Tuning with A Cation

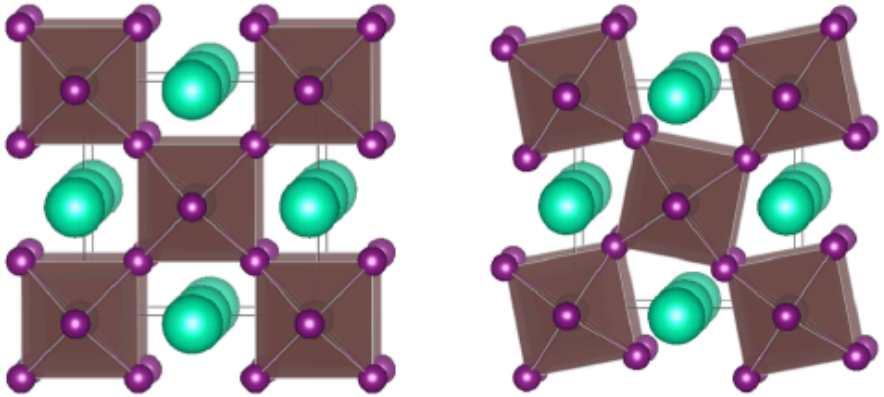

Octahedral Tilting

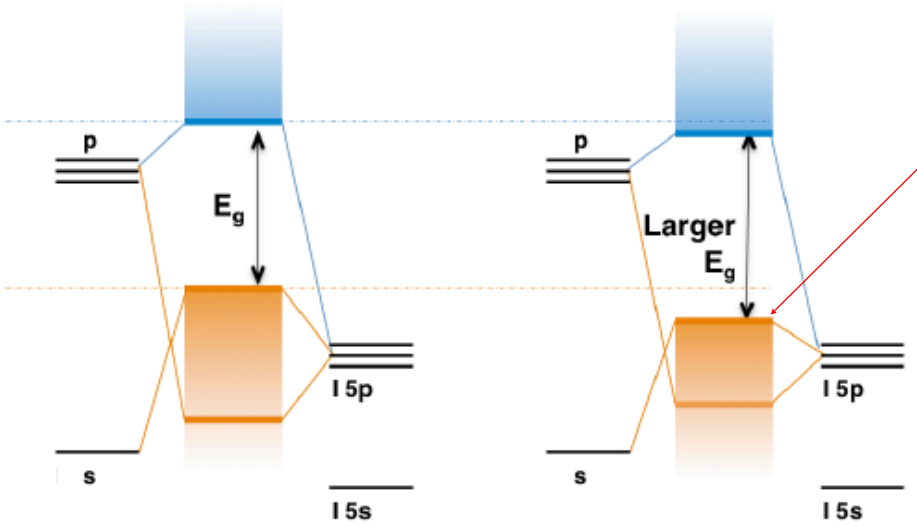

R. Prasanna et al., *J. Am. Chem. Soc.,* **139**, 11117−11124 (2017).

more sensitive to hybridization

R_A: Cs^+ (1.81 Å) < MA^+ (2.70 Å) < FA^+ (2.79 Å)

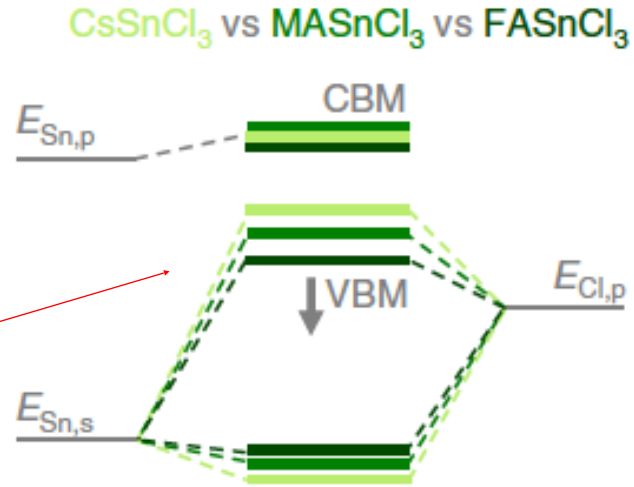

S. Tao et al., *Nature Commun.*, 10:2560 (2019).

- **A-site cations do not directly influence the electronic structure.**
- **Structural deformations (octahedral tilting and distortion) of the octahedra reduce somewhat the hybridization strength between the B and X states: This shifts the VBM and CBM downward.**

History

2009	2012	2013	2014	2015
3.5%	10%	15%	16.5%	20%
Perovskite Dye	Solid state devices	Deposition methods	Solvent Engineering	Composition engineering

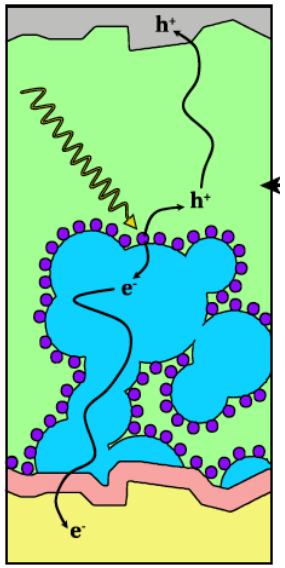

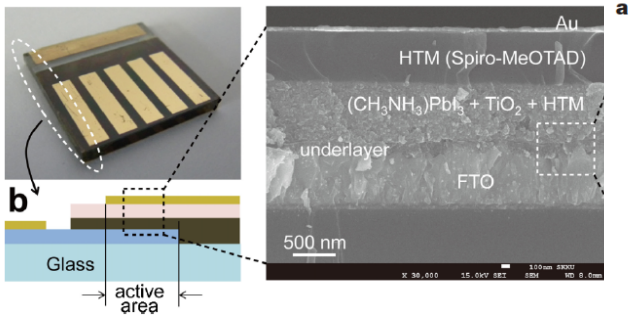

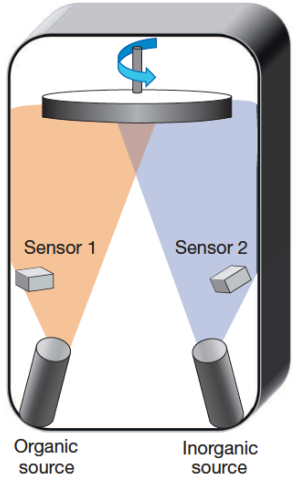

Planar architectures

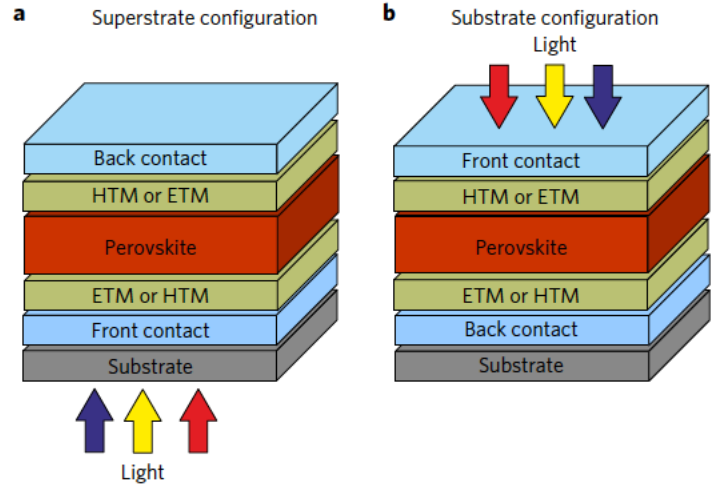

Device Structures

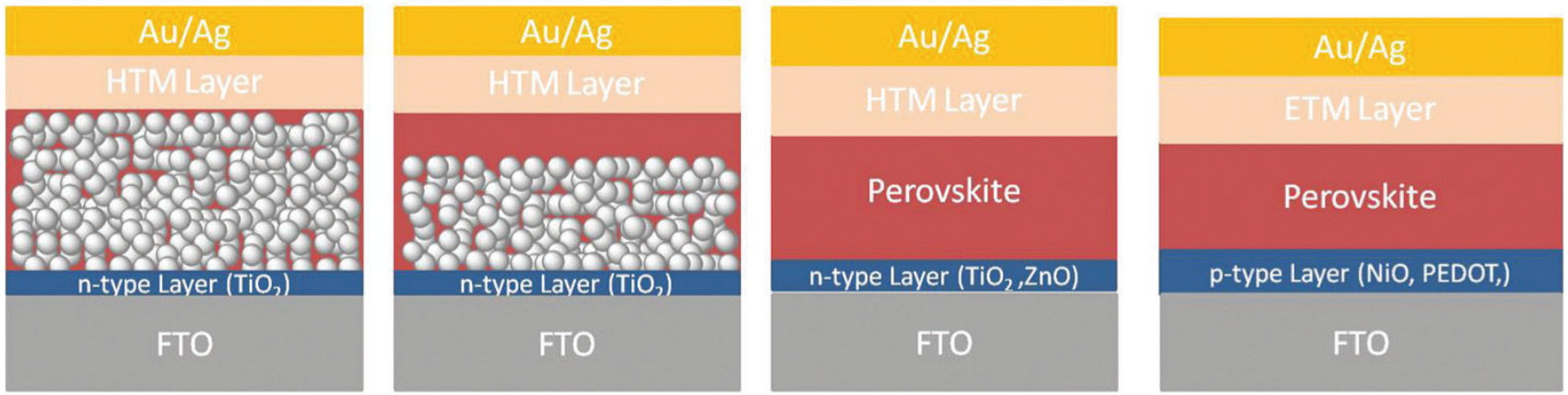

Chem. Soc. Rev., **45**, 655-689 (2016)

TCO: ITO, FTO, etc

Low W_F metal for electron and high W_F metal for hole

ETL (n-type): Inorganic Materials (TiO_2, SnO_2, ZnO, etc) or Organic Materials (PCBM, C60, etc)

HTL (p-type) : Inorganic Materials (NiOx, MoOx, etc) or Organic Materials (Spiro-OMeTAD, PTAA, PEDOT:PSS, etc)

Self-assembled monolayer (SAM): (p-type) MeO-2PACz, 2PACz, (n-type) NI-derivatives

Operation Principle in PSC

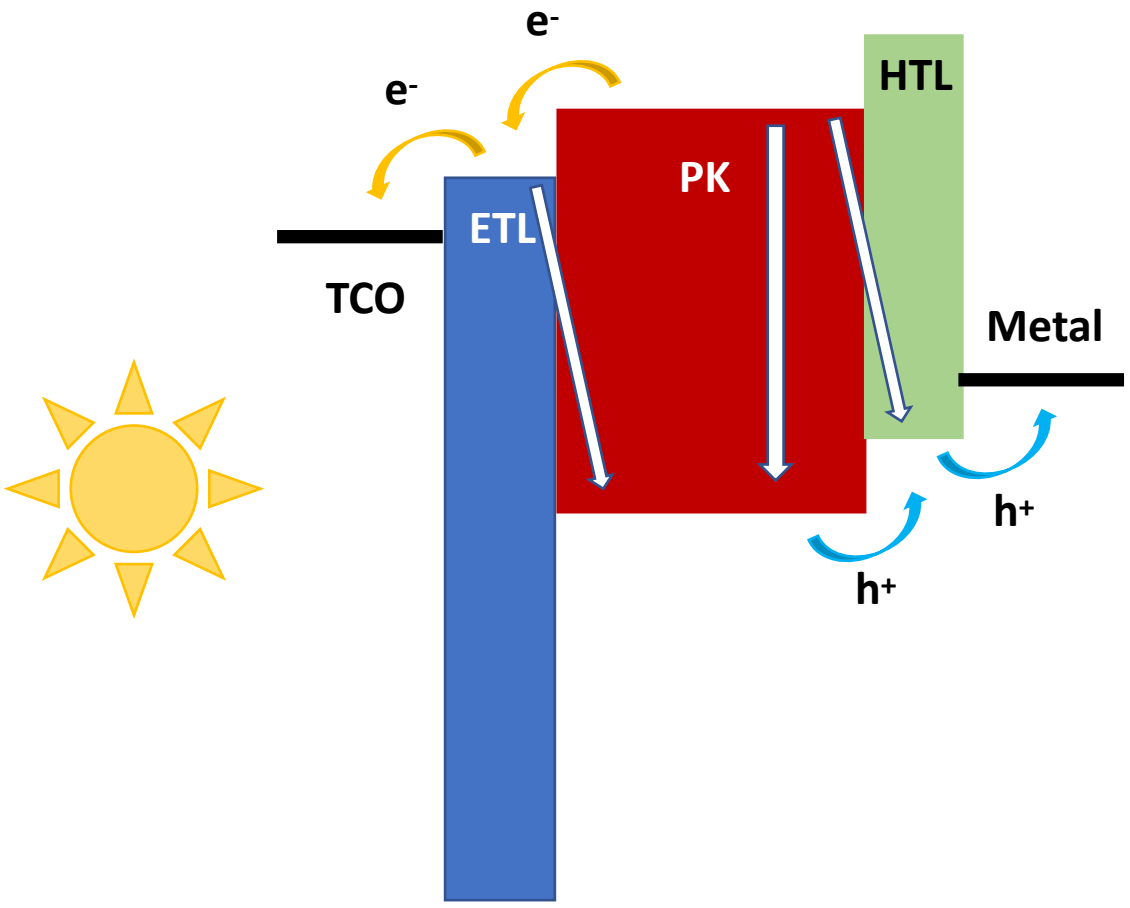

ETL: LUMO or CB lower than CB of perovskite

HTL: HOMO or VB higher than VB of perovskite

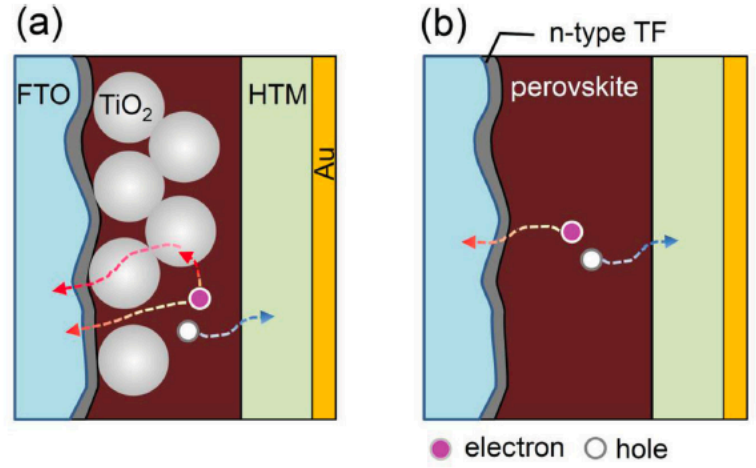

F. Hao et al., , *J. Am. Chem. Soc.*, **136**, 8094 (2014).

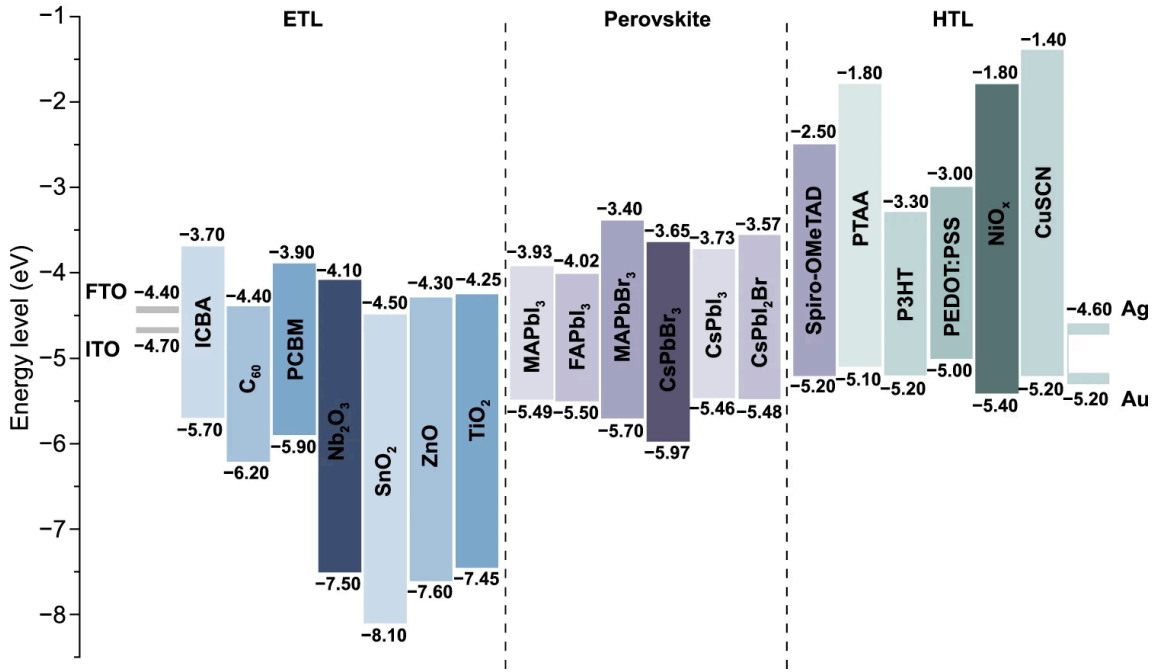

T. Nie et al., *Nano-Micro Lett.*, **15**, 70 (2023).

Device Structures

C60

PCBM

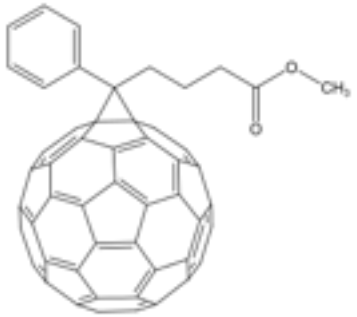

Spiro-OMeTAD

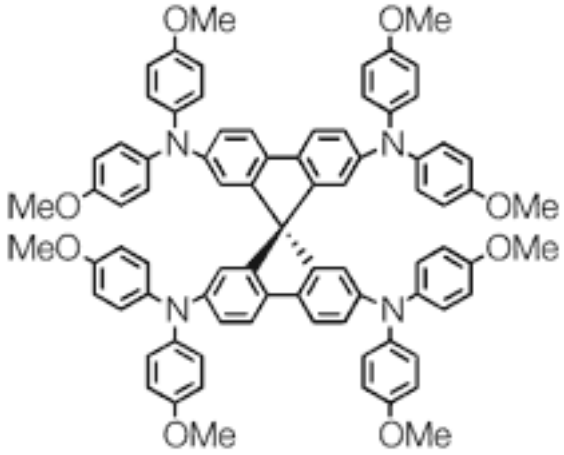

PTAA

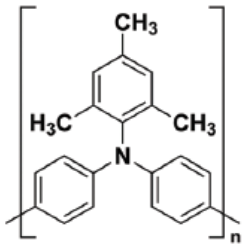

MeO-2PACz

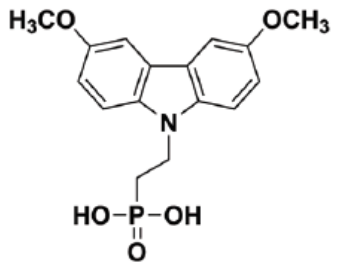

2PACz

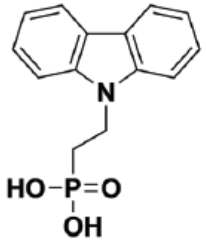

NI

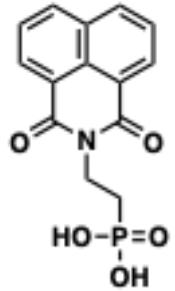

NI-CN

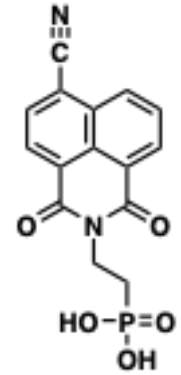

TCO: ITO, FTO, etc

Low W_F metal for electron and high W_F metal for hole

ETL (n-type): Inorganic Materials (TiO_2, SnO_2, ZnO, etc) or Organic Materials (PCBM, C60, etc)

HTL (p-type) : Inorganic Materials (NiOx, MoOx, etc) or Organic Materials (Spiro-OMeTAD, PTAA, PEDOT:PSS, etc)

Self-assembled monolayer (SAM): (p-type) MeO-2PACz, 2PACz, (n-type) NI-derivatives

P. Ferdowsi et al., *Adv. Energy Mater.*, DOI: 10.1002/aenm.202502789 (2025)

Device Structures: SAMs

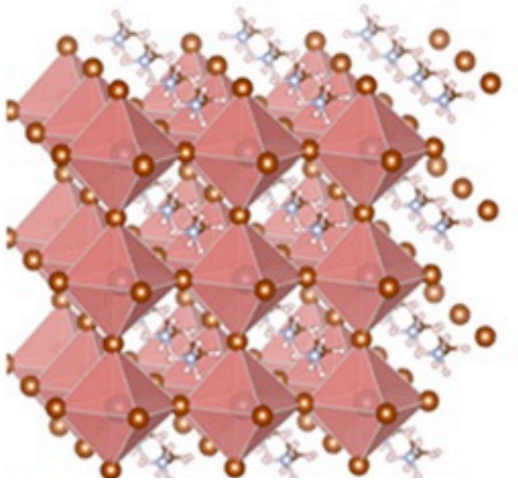

VS

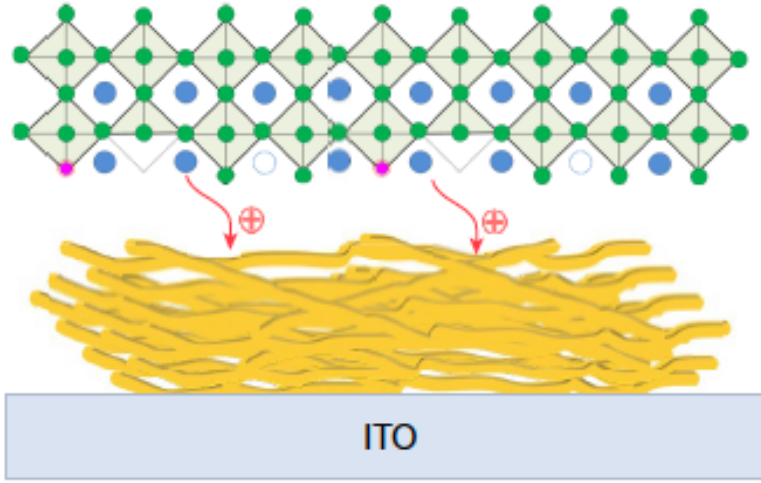

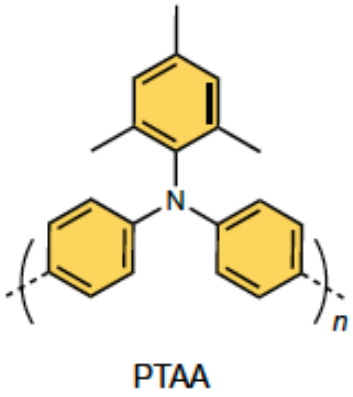

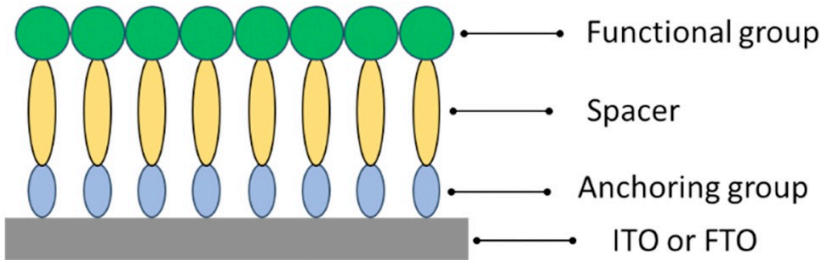

Electron selective layer

Hole selective layer

–COOH, –PO_3H,–SO_3H, –SH, –SiOR

- TCO work function tuning
- Passivation of light active material
- Low parasitic absorption loss
- Low material consumption
- Solution process
- Low temperature process

Device Structures: SAMs

SAM coverage

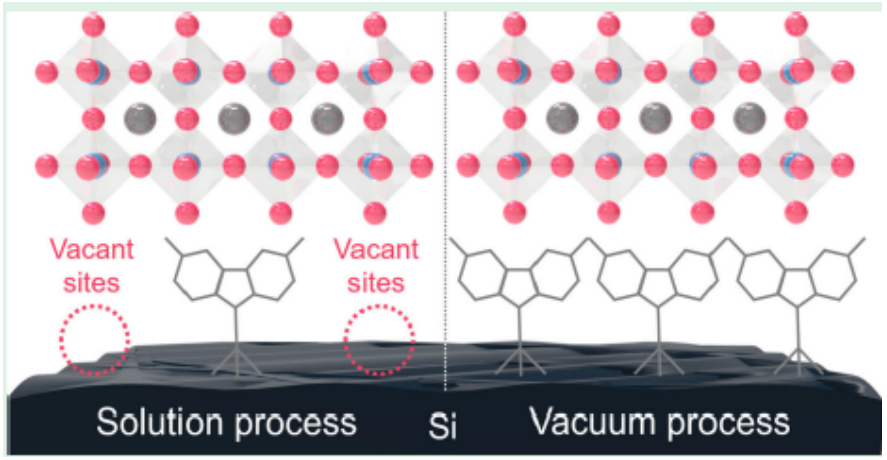

Park et al., *ACS Energy Lett.*, 10, 3743, (2025)

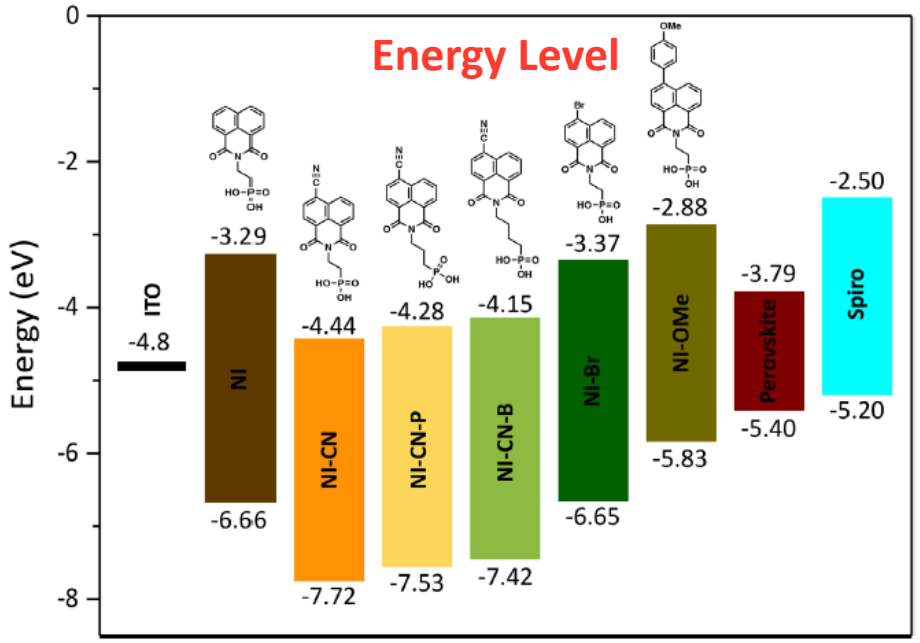

P. Ferdowsi et al., *Adv. Energy Mater.*, DOI: 10.1002/aenm.202502789 (2025)

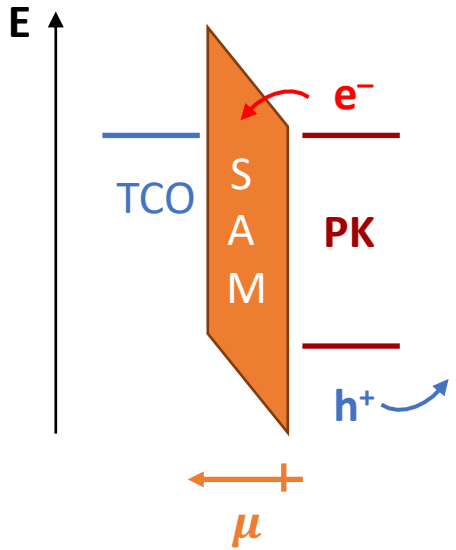

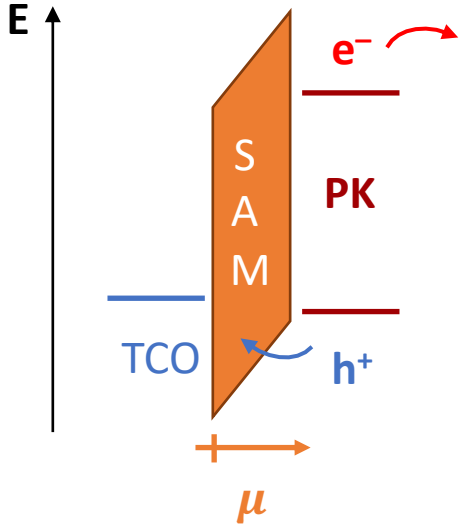

Dipole, Alignment

Conventional Solution Process

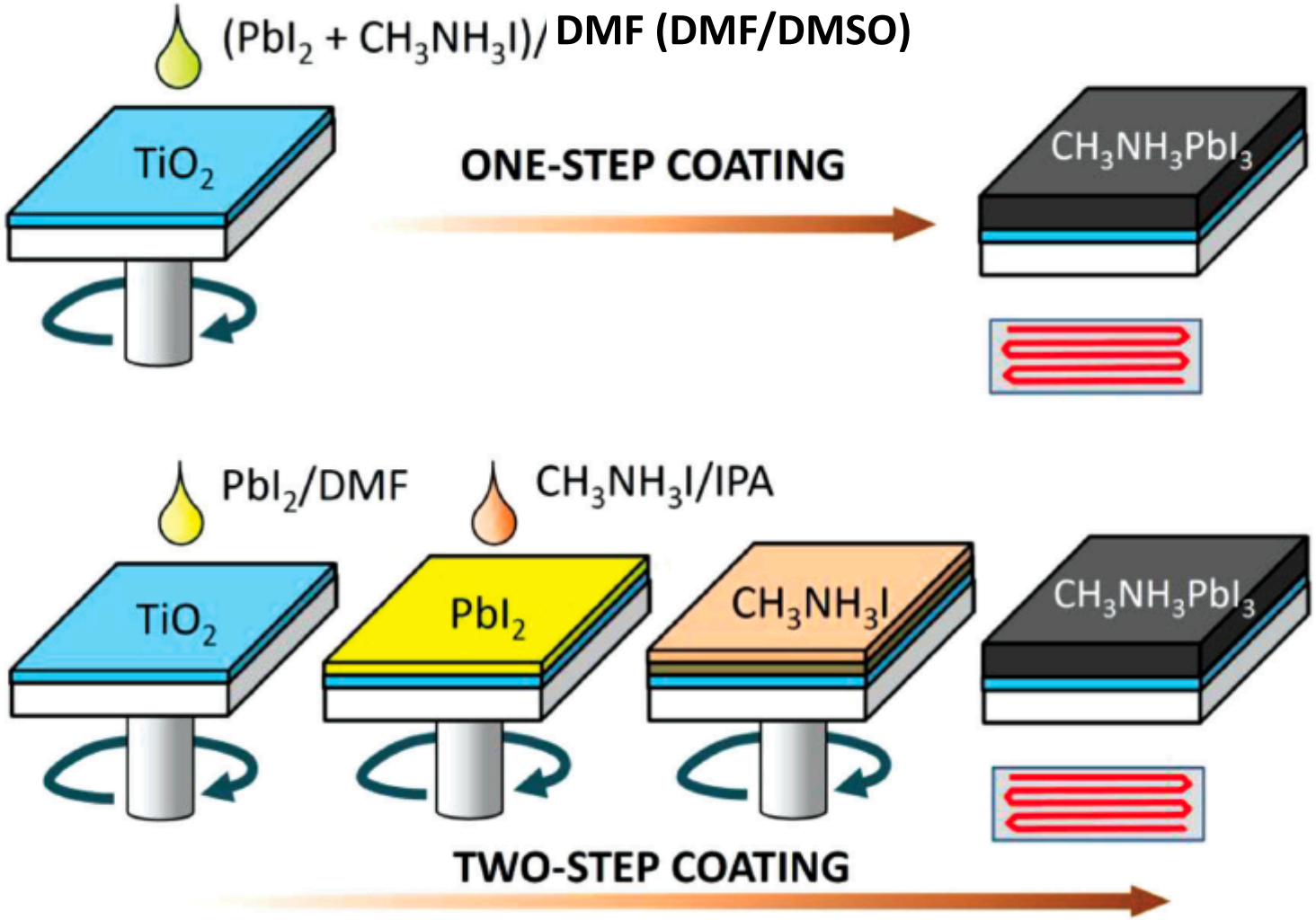

PbI_2, MAI as precursor

DMF: Dimethly Formamide
DMSO: Dimethlysulfoxide
IPA: 2-propanol

F. Hao et al., , *J. Am. Chem. Soc.,* **136**, 8094 (2014).

Antisolvent Method

Antisolvent is **a solvent in which your compound is less soluble.**
Ex) Chlorobenzene, Toluene, Green antisolvents: Diethyl carbonate, n-Ethane etc.

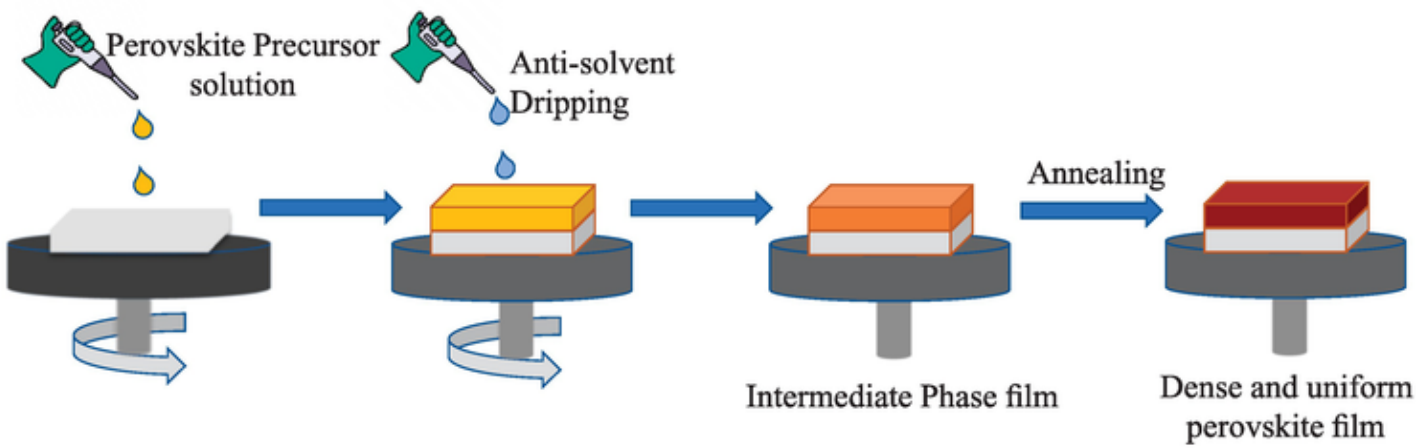

Image taken from "Thin Film Solution Processable Perovskite Solar Cells", IntechOpen, 2022.

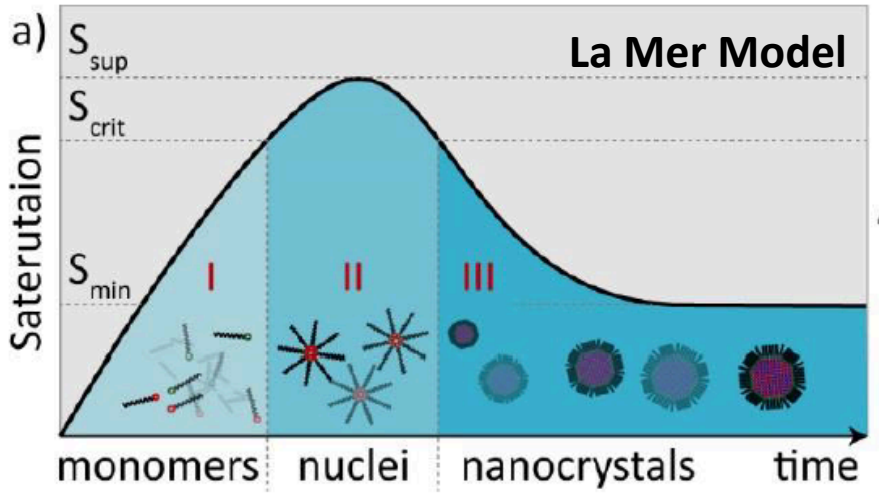

- The principle of antisolvent engineering is **extracting the DMF/DMSO solvent using an antisolvent**.
- This process leads to rapid oversaturation of the components, resulting in the formation of a target perovskite, after low temperature annealing.

Defect Tolerance

- Calculated transition energy levels of various type of point defects in $MAPbI_3$.
- Interstitials (i), vacancies (V), ion substitutions.
- Vacancy type defects produce shallow traps or resonance within the band.
- Some interstitials and substitutions associated with Pb and I form electronic states deep inside the band gap but have relatively high formation energies.

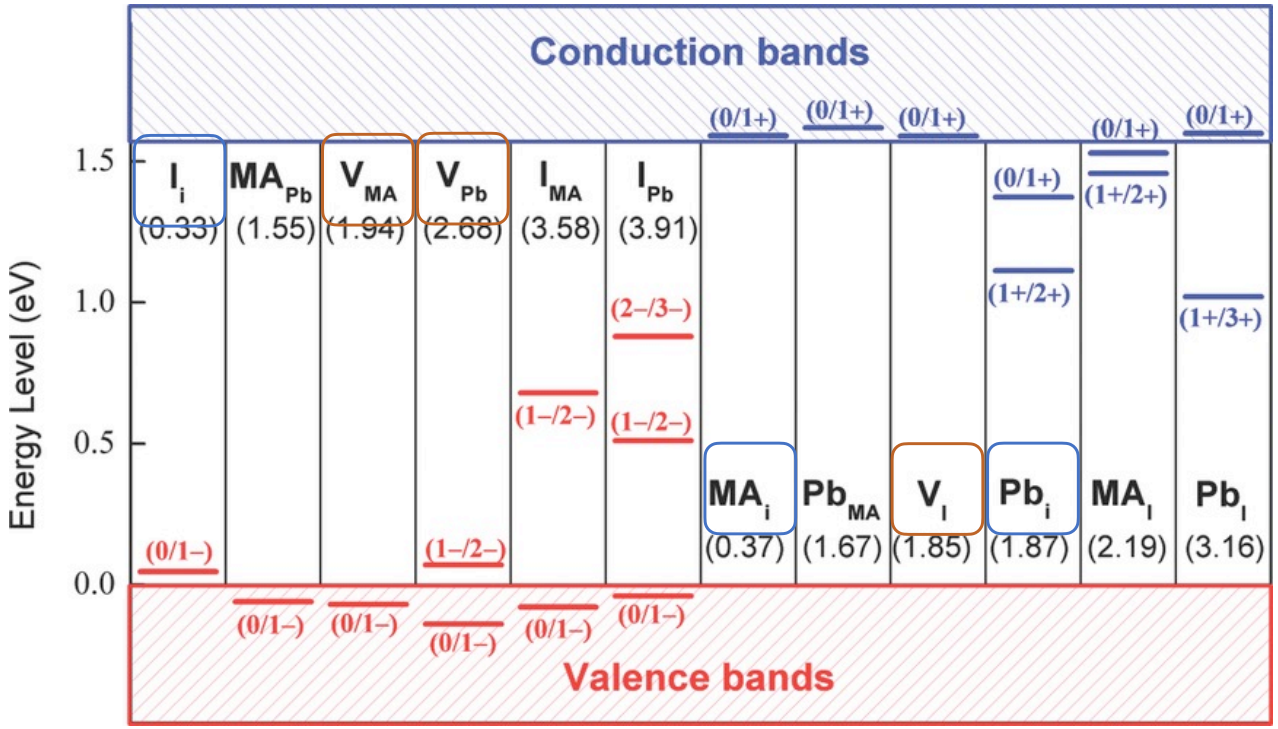

W-J. Yin et al., *Adv. Mater.*, ***26***, 4653–4658 (2014).

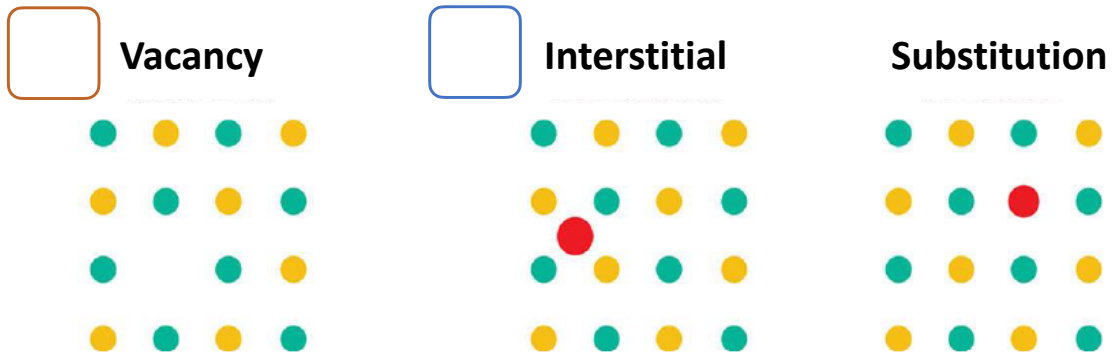

A. Buin et al., *Nano Lett.*, **14**, 6281–6286 (2014).

Towards Higher Performance

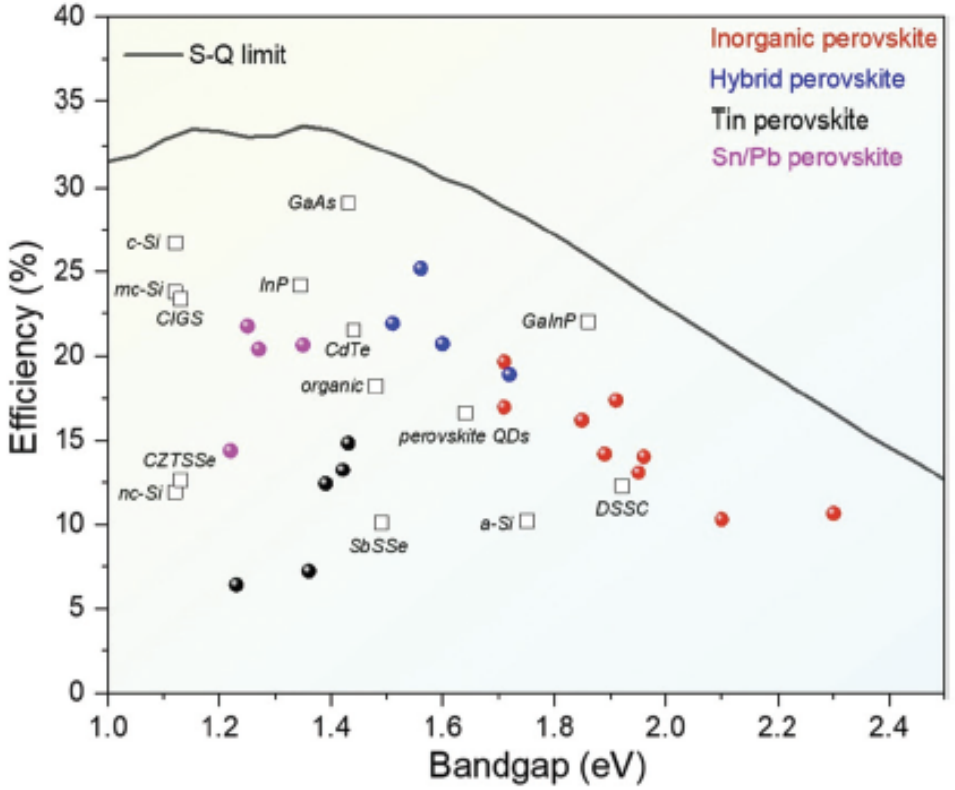

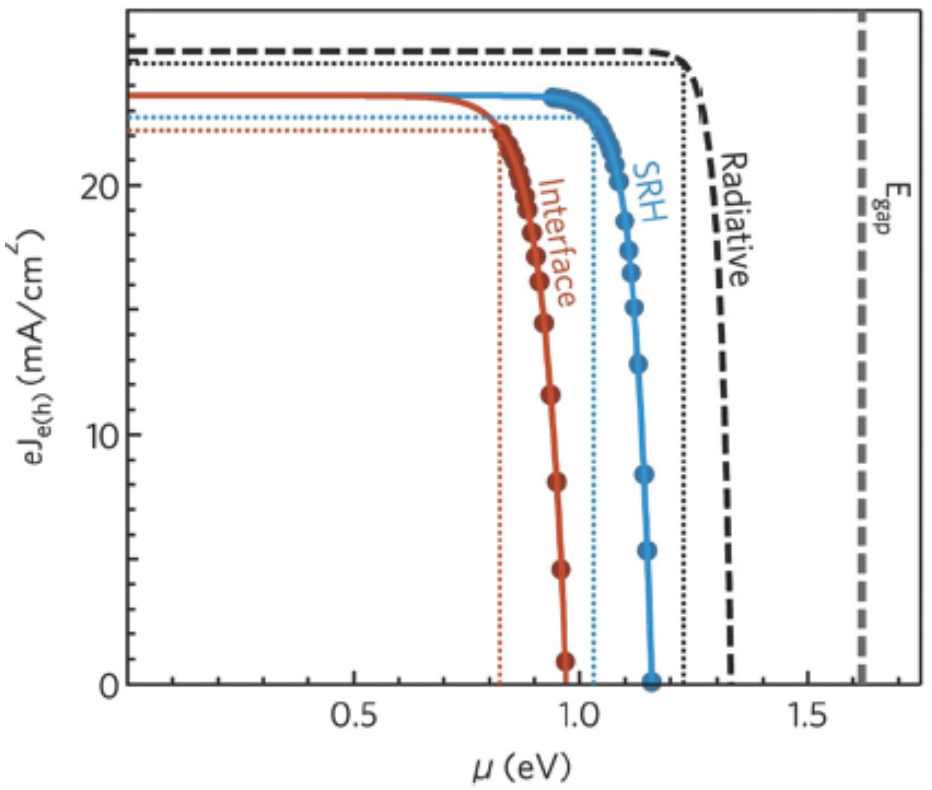

- Impressive efficiencies **over 25%** have been achieved.
- Room for further improvement.
- SRH non-radiative recombination by deep and shallow defects : film quality, crystal size, passivation.
- Interface recombination: energy alignment, charge extraction.
- Career management → enhanced V_{oc}, J_{sc} and *FF*.
- Light management → enhanced J_{sc}.

Image taken from Z. Guo et al., *Energy Environ. Sci.*, **15**, 3171 (2022)

Stability & Hysteresis

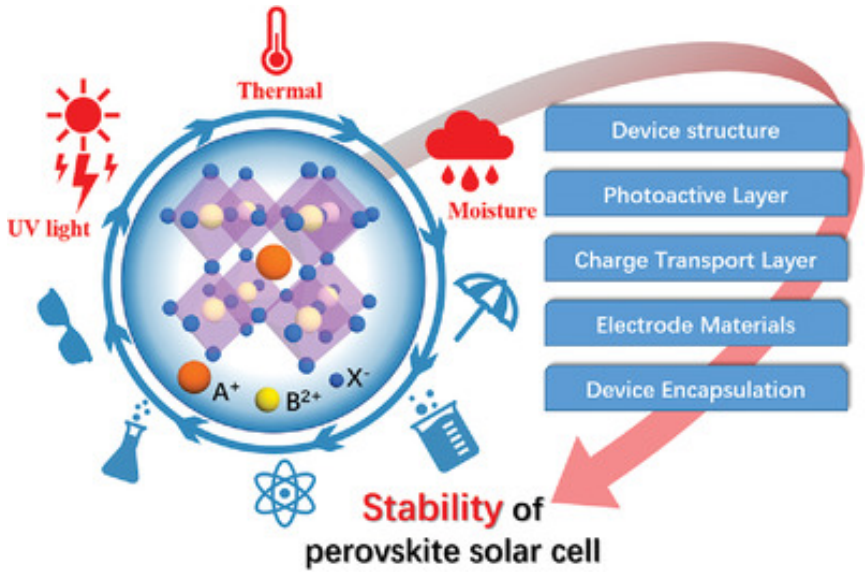

R. Wang et al., *Adv. Funct. Mater.*, **29**, 1808843 (2019)

- The hydrogen bond between organic (-NH_3^+) and inorganic units: weak by the high polarity of a water molecule.

$$CH_3NH_3PbI_3 \text{ —> } PbI_2 + CH_3NH_3I$$

under ambient condition

- The decomposition temperature of $CH_3NH_3PbI_3$ has been reported as being between 100 and 140 °C.

$$CH_3NH_3PbI_3 \text{ —> } PbI_2 + CH_3NH_3 + HI$$

- UV light possibly induces the formation of defects, particularly in the presence of oxygen and iodide vacancies.

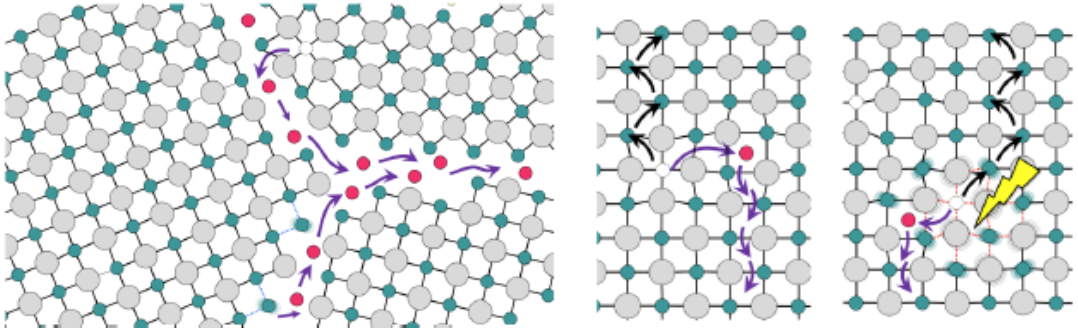

Y. Yuan et al., *Acc. Chem. Res.*, **49**, 286 (2016)

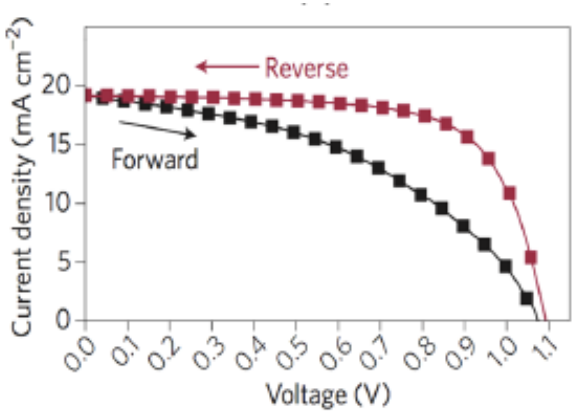

- Current–Voltage hysteresis
- Phase segregation (pristine, I-rich. Br-rich)

Beyond S-Q Limit

- **Tandem Solar Cells**
- **Concentrated Solar Cells**
- **Intermediate Band Solar Cells**
- **Hot Carrier and Carrier Multiplication**

Tandem Solar Cells

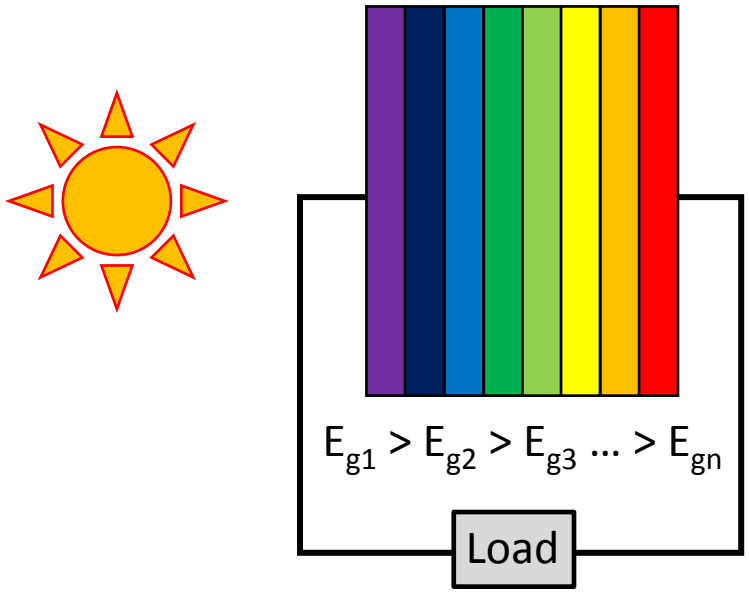

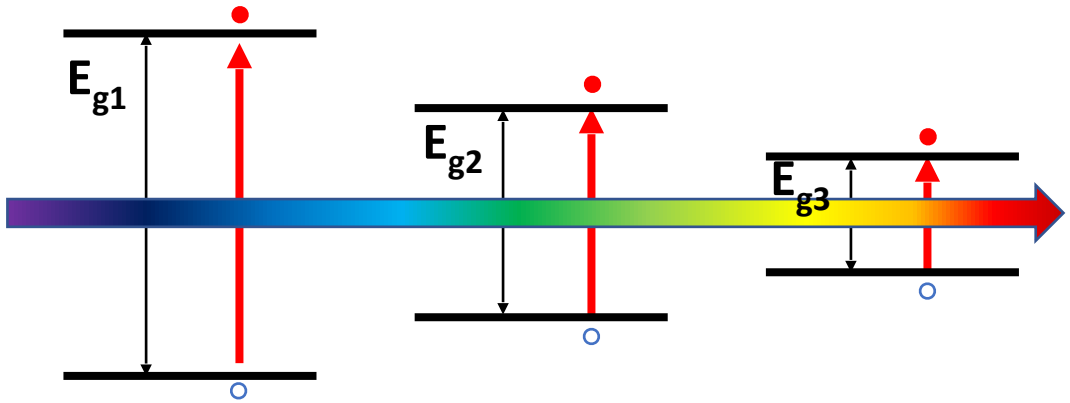

- **$V = V(E_{g1}) + V(E_{g2}) + V(E_{g3})$**
- **J is determined by the lower value**

Tandem solar cells: Semiconductors with different bandgaps connected electrically in series either in the same device or in different devices.

Efficiency can be significantly enhanced by using a stack of materials with different band gaps.

- **Efficiency >45% (dual junction)** is possible under standard AM 1.5 illumination.
- **Challenges**:
  - Current matching required for series connection of junctions. Sensitive to illumination conditions.
  - Difficult to maintain a high crystal quality due to lattice mismatch.
  - High cost.

Tandem Solar Cells

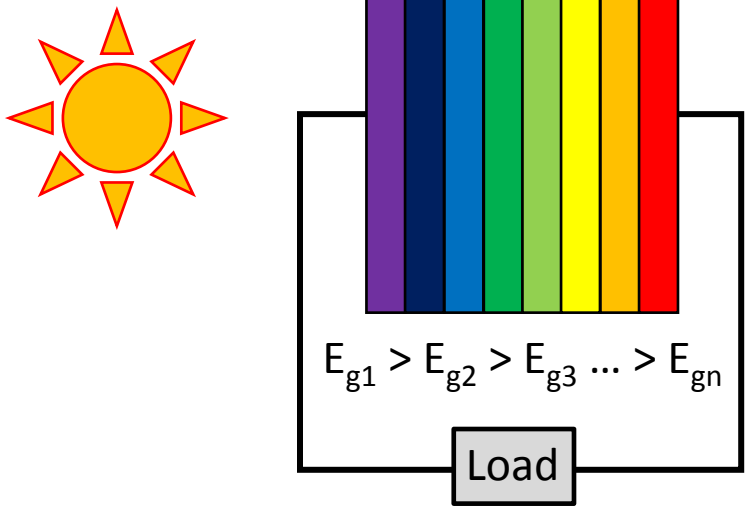

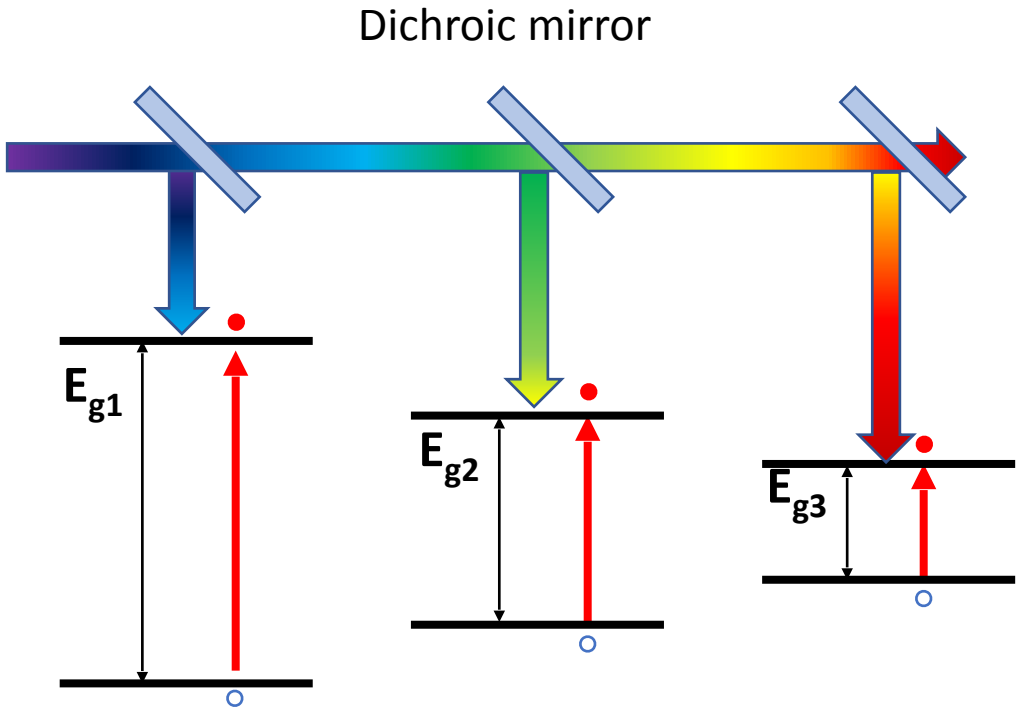

Tandem solar cells: Semiconductors with different bandgaps connected electrically in series either in the same device or in different devices.

Efficiency can be significantly enhanced by using a stack of materials with different band gaps.

- **Efficiency >45% (dual junction)** is possible under standard AM 1.5 illumination.
- **Challenges**:
  - Current matching required for series connection of junctions. Sensitive to illumination conditions.
  - Difficult to maintain a high crystal quality due to lattice mismatch.
  - High cost.

Tandem Solar Cells

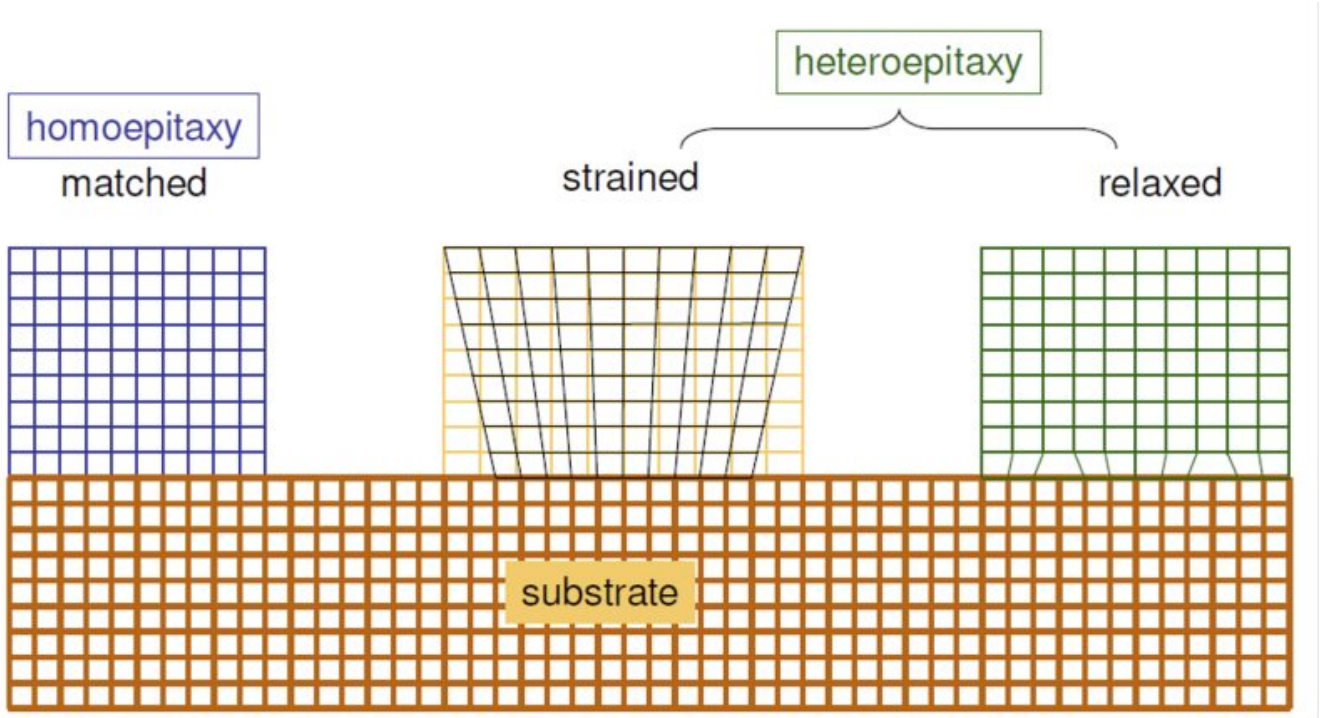

Image taken from https://www.mks.com/n/silicon-epitaxial-thin-films

- Epitaxy is defined as the "regularly oriented growth of one crystalline substance on another".
- Lattice mismatch, $\varepsilon < 0.4\%$, is necessary for obtaining high quality epitaxy.

$$\varepsilon = \frac{a_f - a_s}{a_f}$$

a_f: lattice constant of the film

a_s: lattice constant of the substrate

Tandem Solar Cells

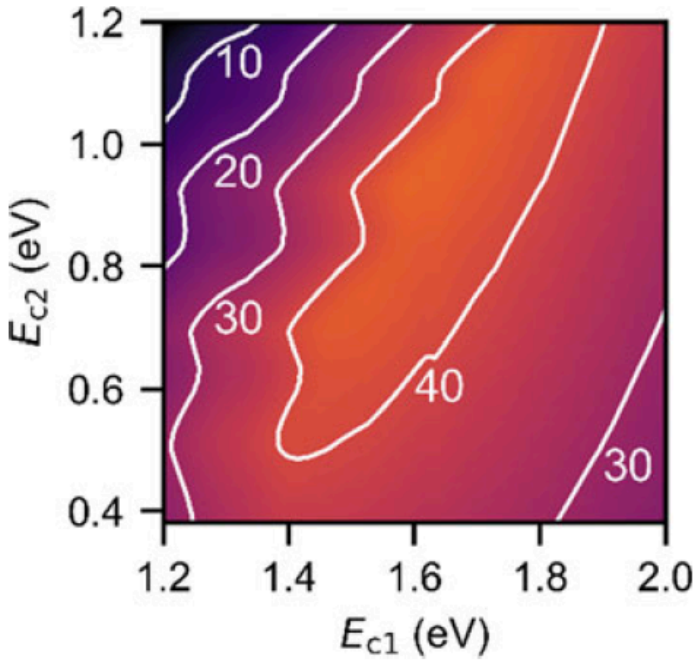

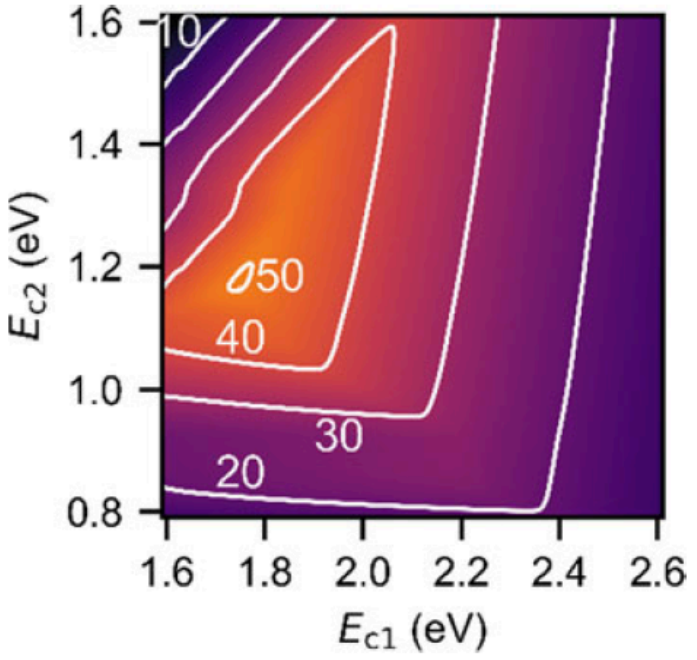

A **dual junction solar cell**:
At the point E_{c1} = 1.58 eV and E_{c2} = 0.94 eV, the conversion efficiency reaches its maximum of **45.4%**.

A **triple junction solar cell**:
With Ge (E_{c3} = 0.66 eV), at the point E_{c1} = 1.76 eV and E_{c2} = 1.18 eV, the conversion efficiency reaches its maximum of **50.3%**.

Image taken from Energy Conversion Efficiency of Solar Cells, Springer

III-V Semiconductors: Multijunction Solar Cells

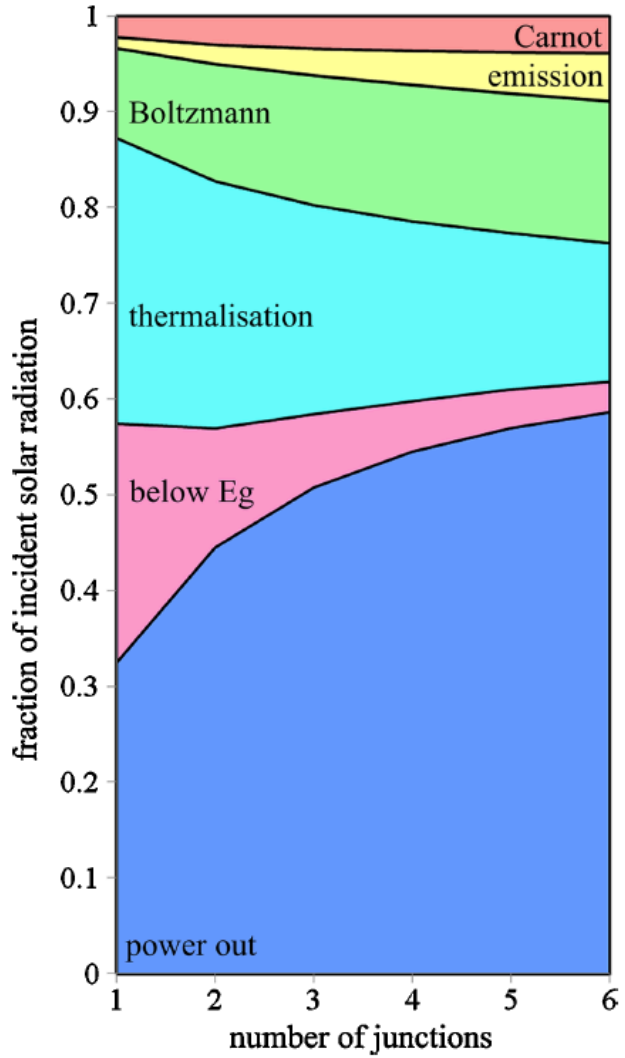

Hirst et al., *Prog. Photovolt: Res. Appl.*, **19**, 286–293 (2011)

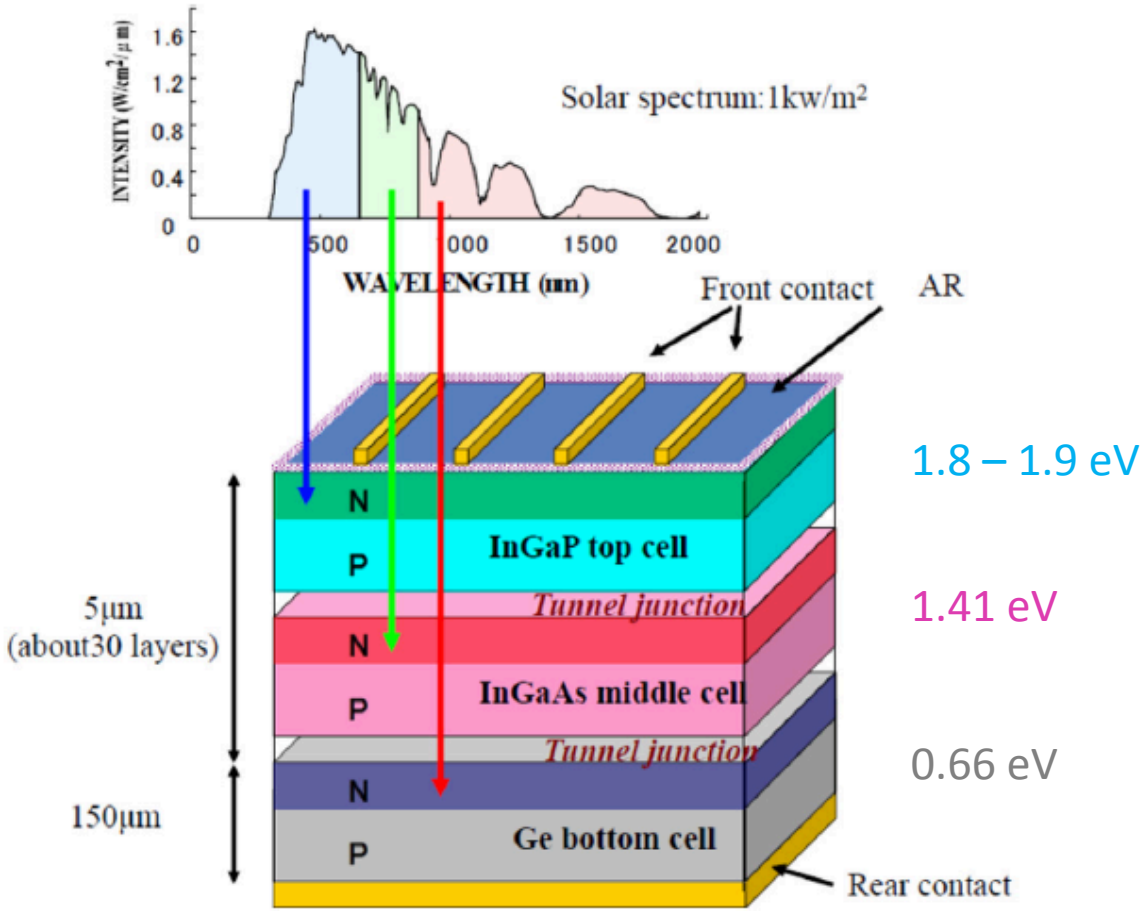

Yamaguchi et al., *J. Appl. Phys.*, **129**, 240901 (2021)

III-V Semiconductors: Multijunction Solar Cells

η = **39.2 %** under the 1-Sun global spectrum (AM1.5G)

η = **47.1 %** under the direct spectrum (AM1.5D) under 143 Suns concentration

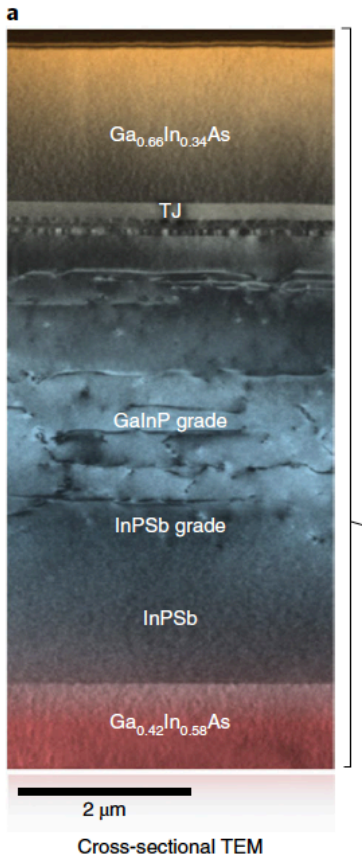

Cross-sectional TEM

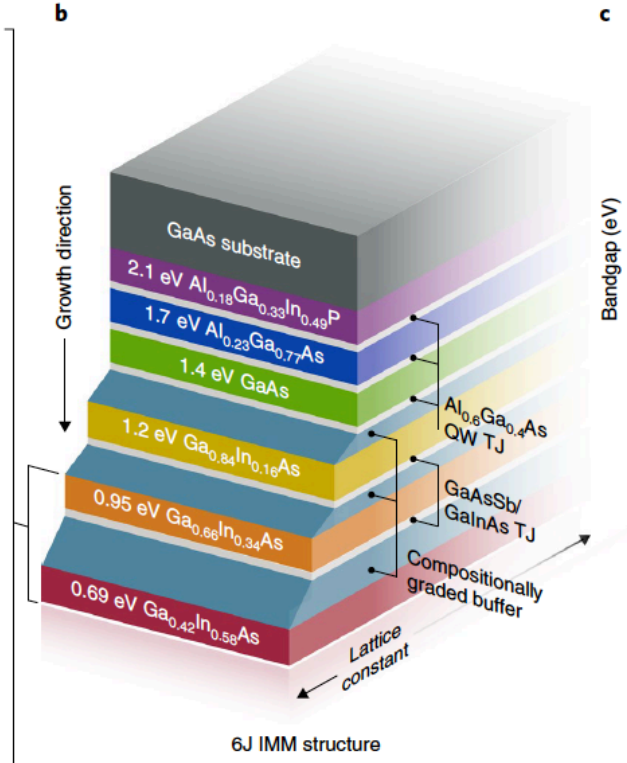

6J IMM structure

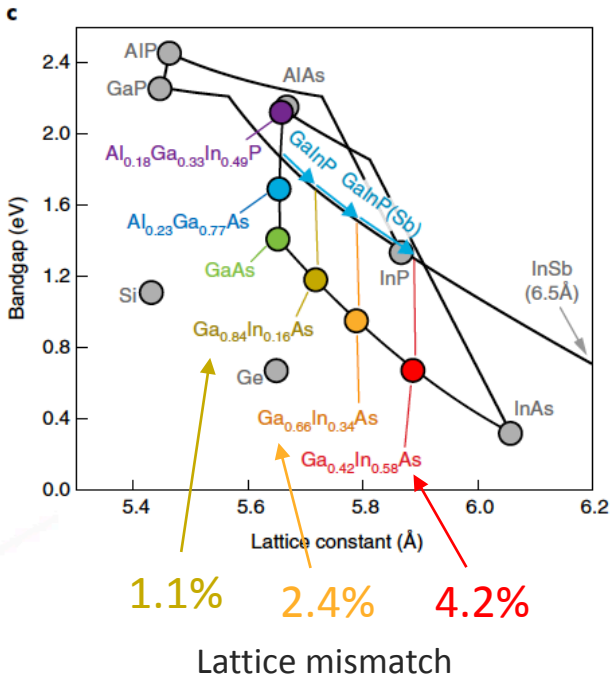

Lattice mismatch

Geisz et al., Nature Energy, 5, 3226 – 335 (2020)

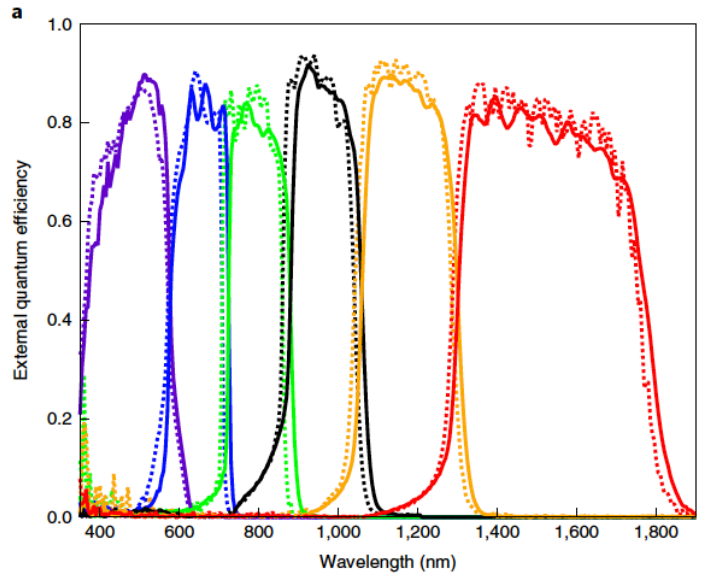

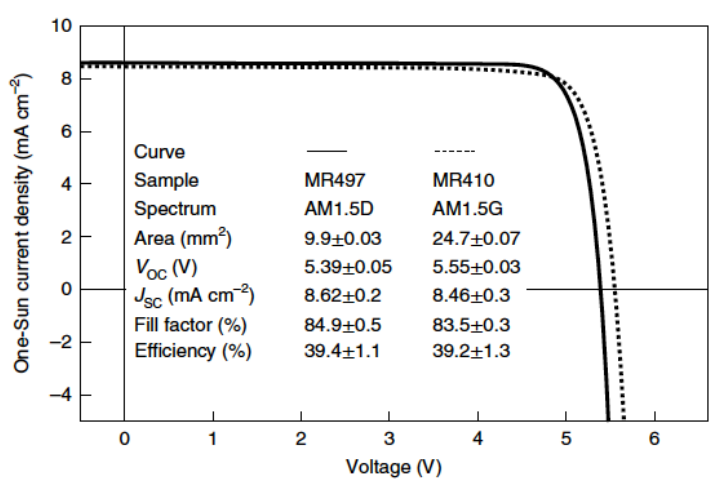

Halide Perovskite is Ideal for Tandem Solar Cells?

- **Optical bandgap: 1.57 eV**
- **Band gap Tuning**
- **No optically detectable deep states.**
- **Highest reported V_{oc} values:**

  c-Si = 0.75 V, GaAs = 1.12 V, $CH_3NH_3PbI_3$ = 1.05 V.

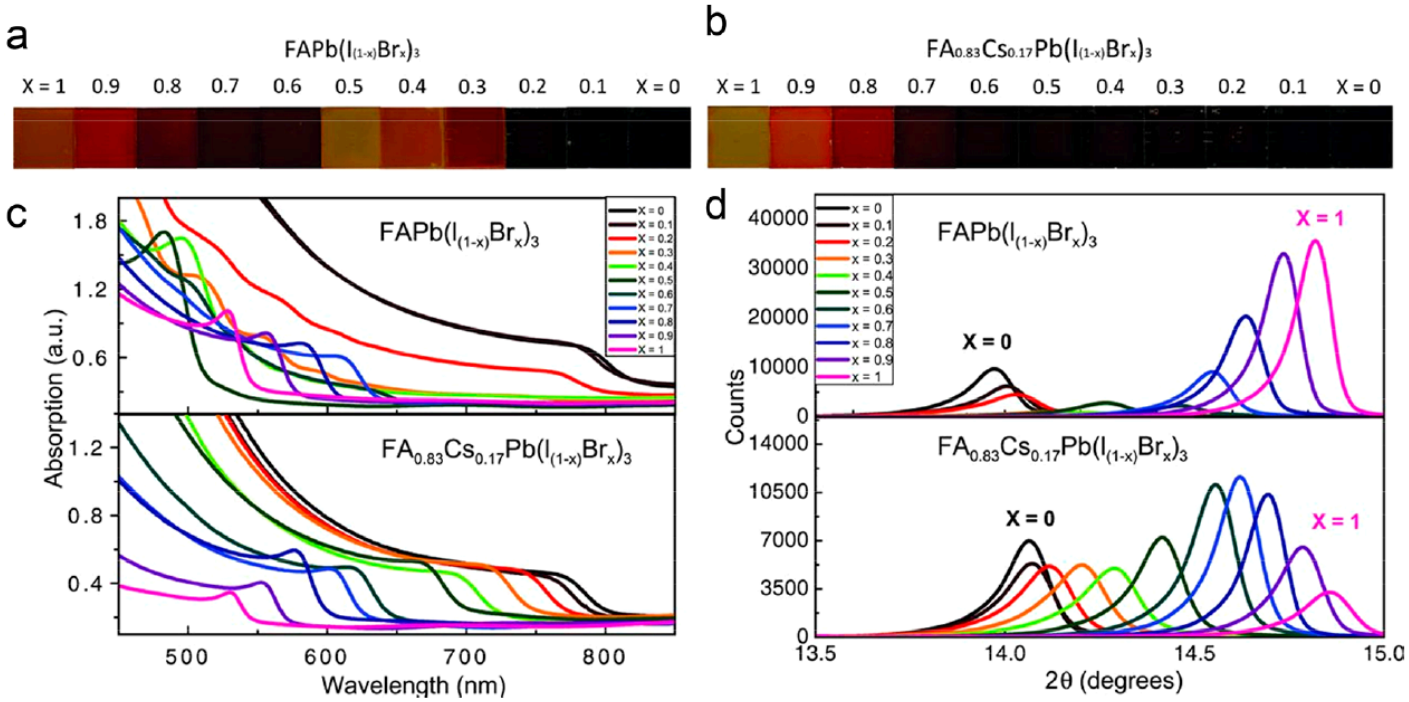

D. P. McMeekin, *Science*, **351**, 151−155 (2016).

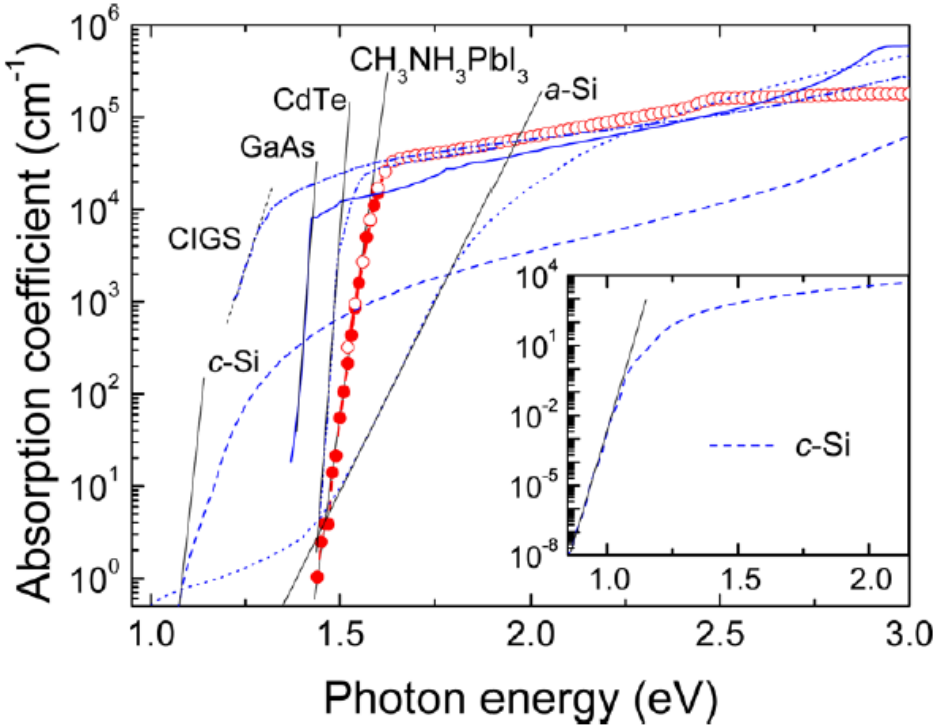

S. De Wolf et al., *J. Phys. Chem. Lett.*, **5**, 1035−1039 (2014).

Perovskite/Si Tandem Solar Cell

Tandem cells at 34.85%

LONGi have set a new world efficiency record for its perovskite/silicon tandem solar cells.

https://www.longi.com/en/news/silicon-perovskite-tandem-solar-cells-new-world-efficiency/

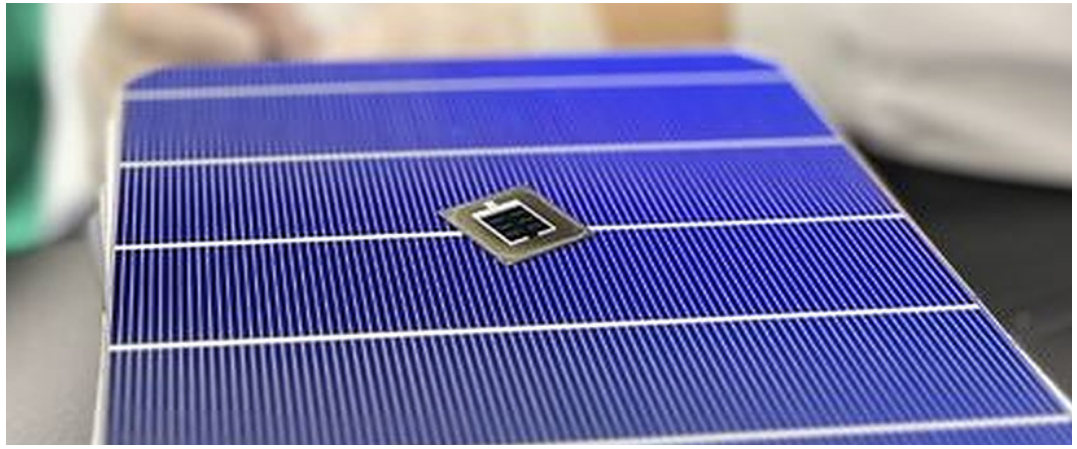

III-V/Si

Perovskite/Si

Perovskite/CIGS

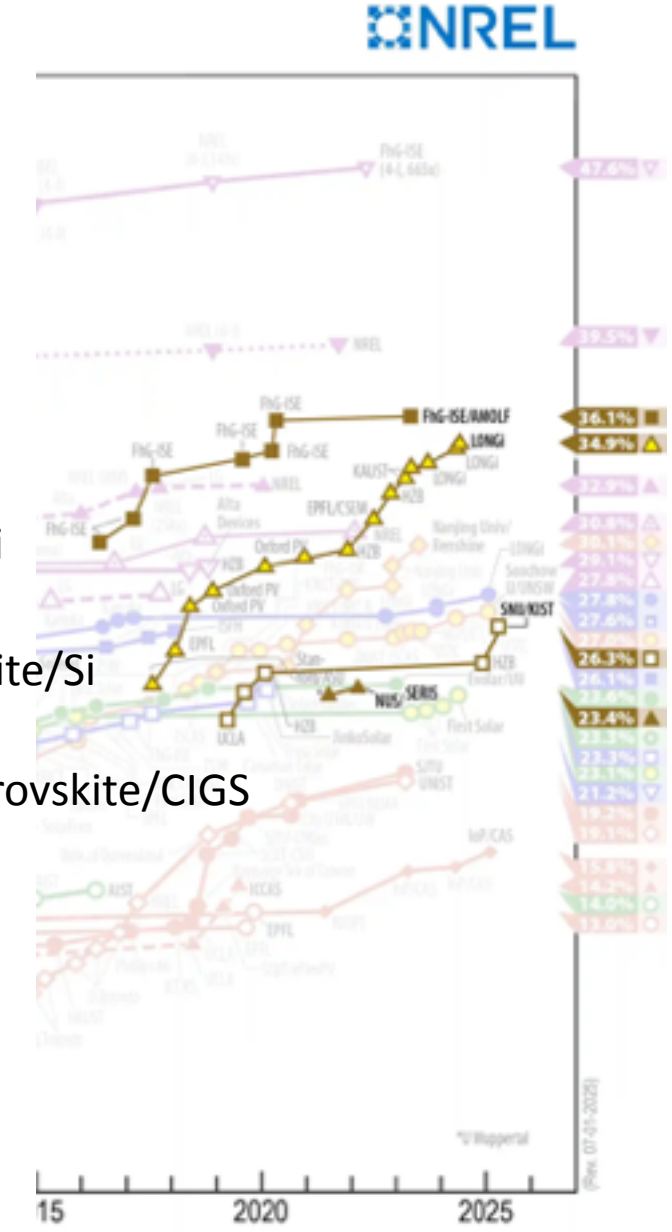

Concentrated Solar Cells

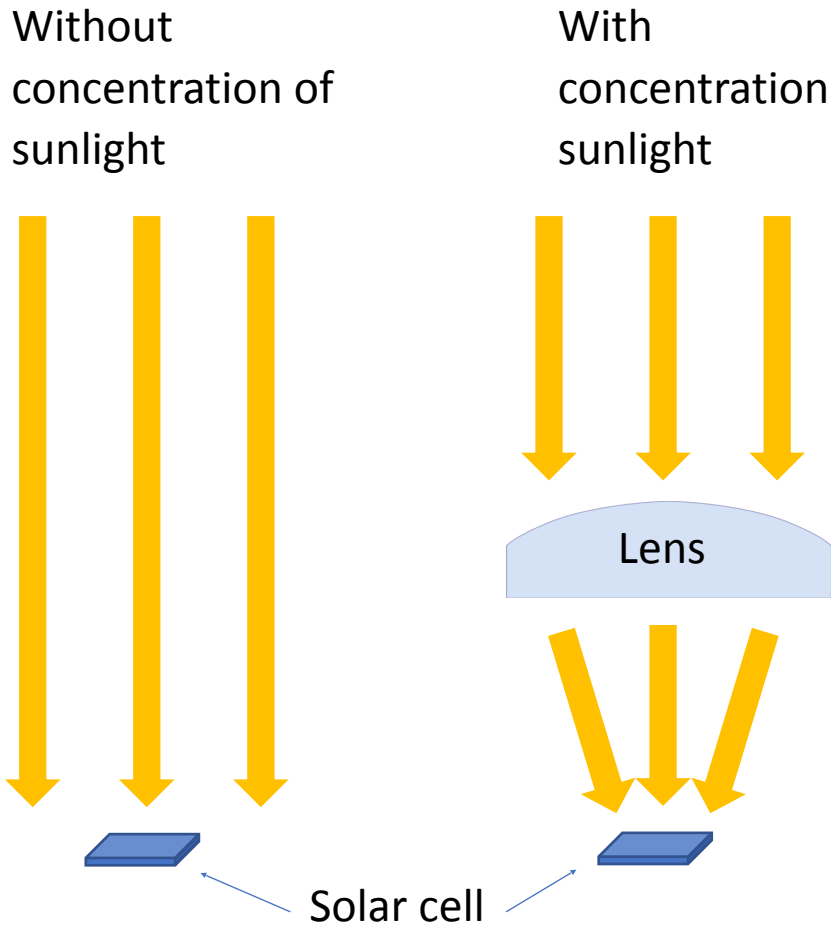

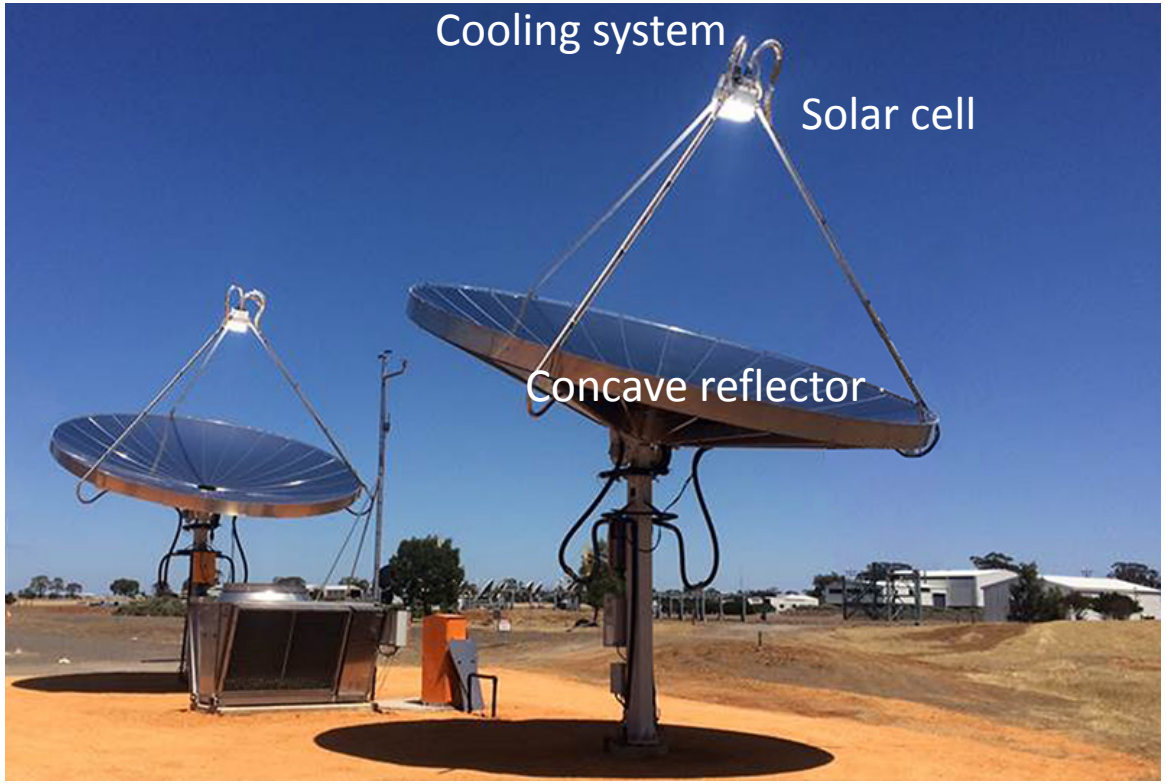

Concentrated Solar Cells

J_{SC} is proportional to incident optical power density

V_{OC} increases logarithmically with J_{SC}.

$$V_{OC}(C \times J_{SC}) = \frac{k_B T}{q} \times \ln\left(C \times \frac{J_{SC}}{J_0}\right) = V_{OC}(J_{SC}) + 0.26 \times \ln(C) \qquad C = concentration\ factor$$

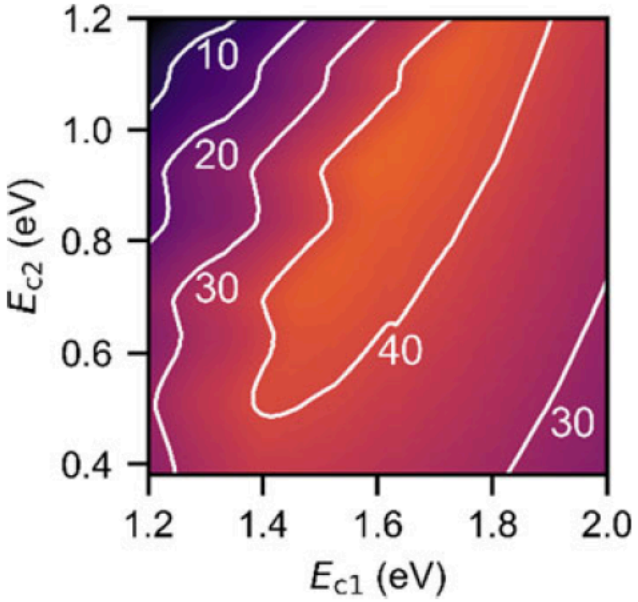

The conversion efficiency of the dual-junction solar cell under **unconcentrated light (45.4%)**.

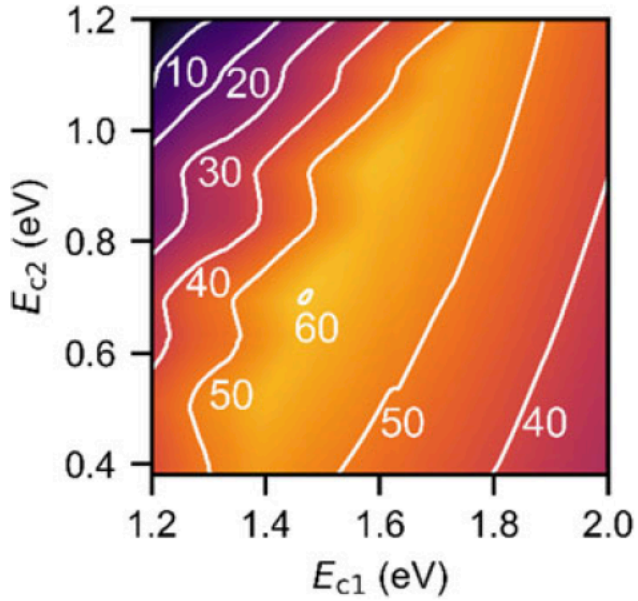

The conversion efficiency of the dual-junction solar cell under **concentrated light (C = 1000)** and it reaches the maximum of **60%** at E_{c1} = 1.44 eV and E_{c2} = 0.70 eV.

III-V Semiconductors: Multijunction Solar Cells

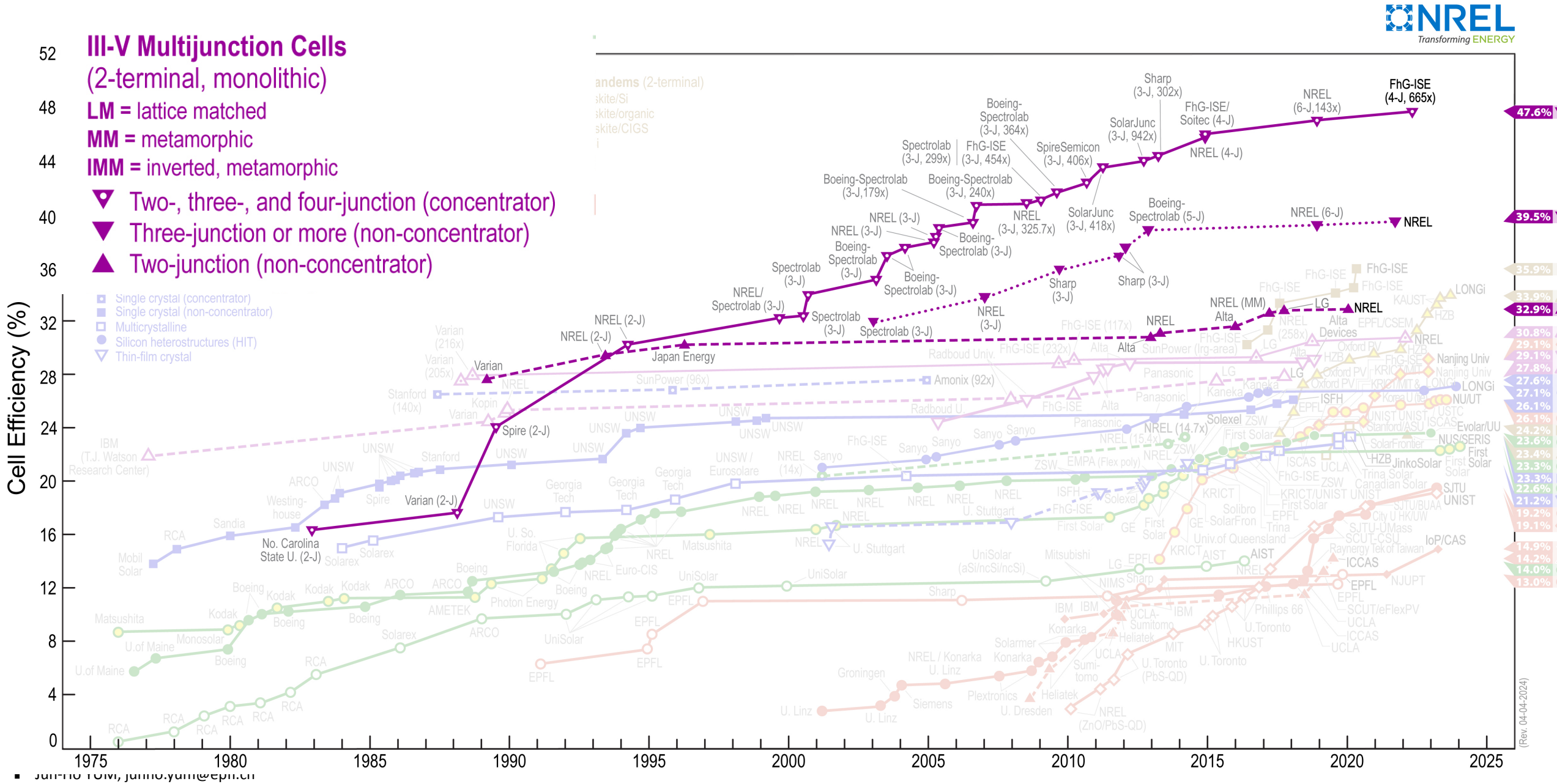

- Jun-Ho YUM, junho.yum@epfl.ch

Intermediate-band Solar Cells

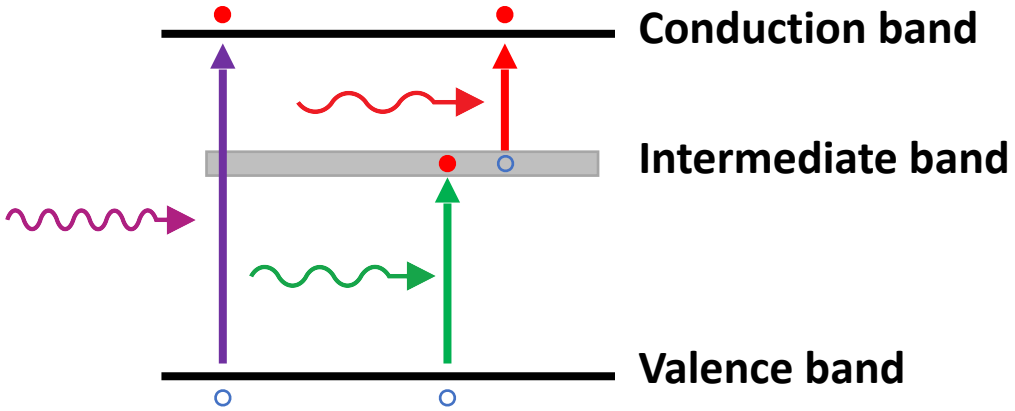

Less sensitive to illumination condition due to the direct absorption via inter-band transition and a stepwise absorption via the intermediate band.

$$I_{total} = I_{VC} + I_{IC}$$

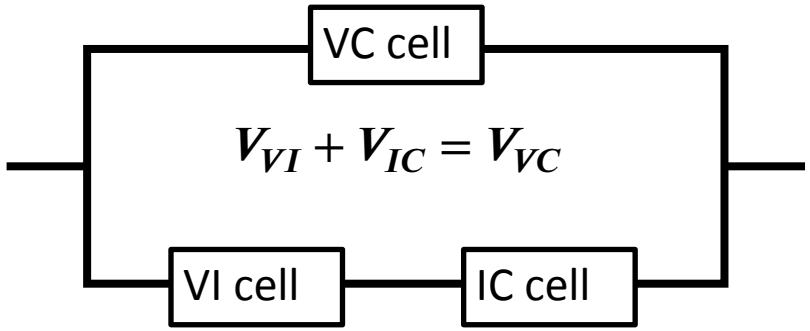

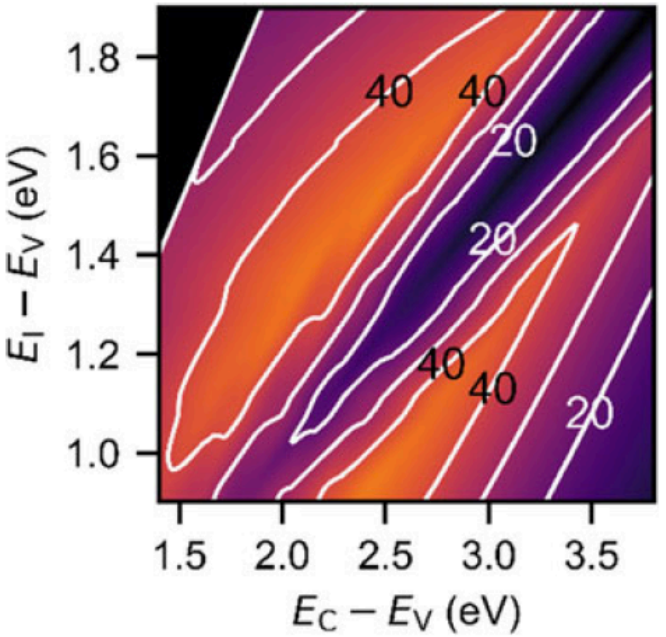

A maximum conversion efficiency of **49.4%** is reached for a band-gap energy of 2.43 eV between the CB and the VB, and an energy gap of 1.49 eV between the valence band maximum (VBM) and the intermediate-band quasi-Fermi level.

Hot Carrier Generation and Carrier Multiplication

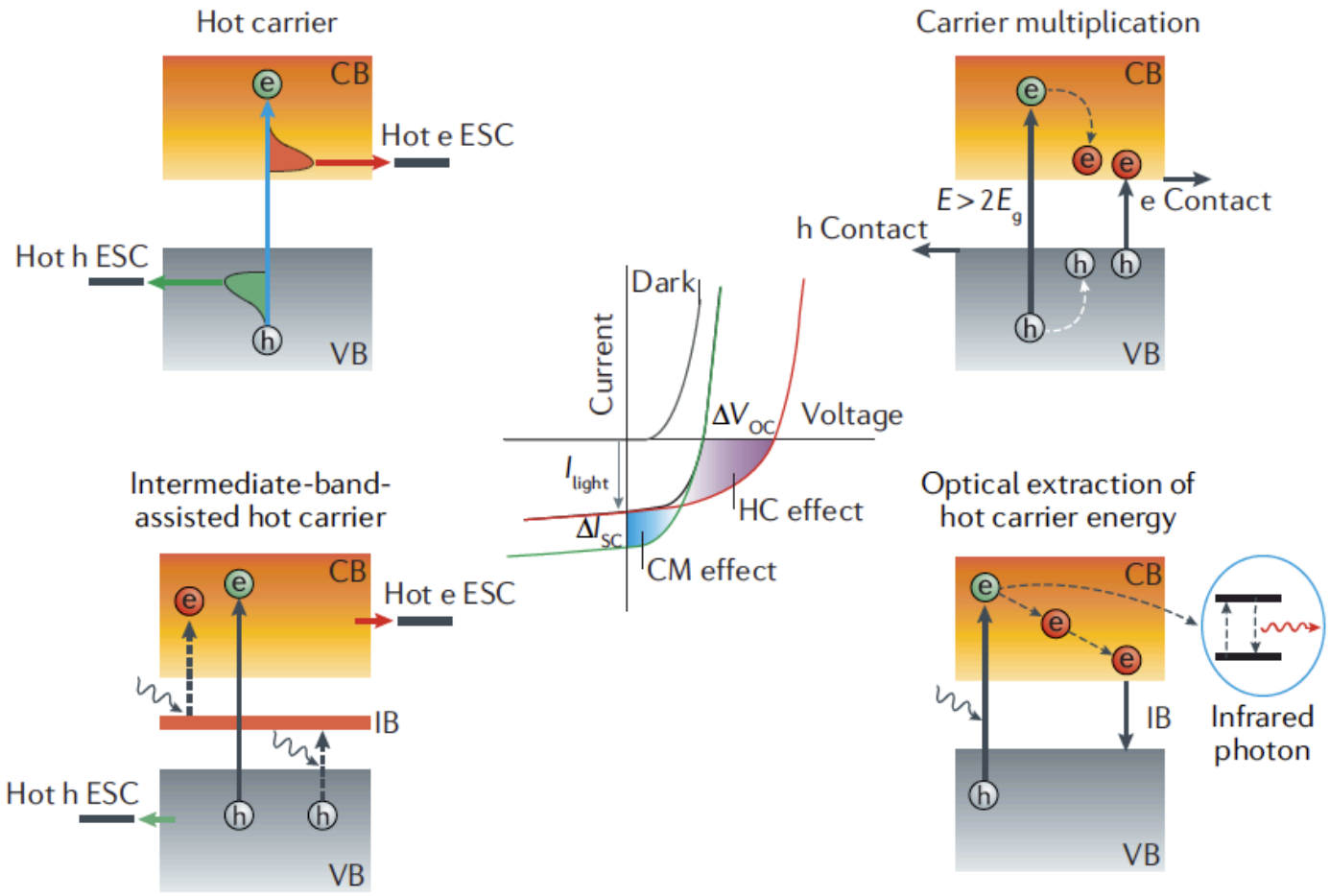

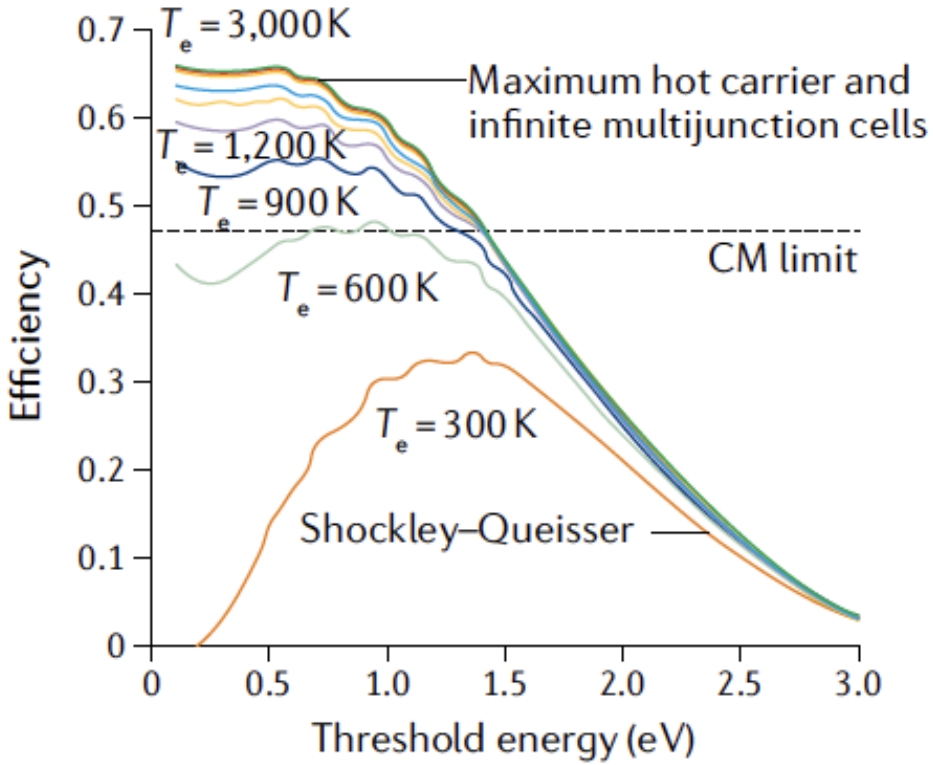

ESC: energy- selective contacts

Images taken from K. K. Paul et al., *Nature Reviews Physics*, **3**, 178 (2021)